Title

A genetic basis for molecular asymmetry at vertebrate electrical synapses

Authors

Adam C Miller[1,2], Alex C Whitebirch[1,3], Arish N Shah[3], Kurt C Marsden[4], Michael Granato[4], John O'Brien[5], and Cecilia B Moens[3]

[1] Co-first authors.

Affiliations

[2] Institute of Neuroscience, University of Oregon, Eugene, OR, USA.

[3] Division of Basic Sciences, Fred Hutchinson Cancer Research Center, Seattle, WA, USA.

[4] Department of Cell and Developmental Biology; University of Pennsylvania Perelman School of Medicine; Philadelphia, PA, 19104, USA.

[5] Department of Ophthalmology and Visual Science, McGovern Medical School, University of Texas Health Sciences Center at Houston; Houston, TX, 77225, USA.

Corresponding author

Adam Miller, acmiller@uoregon.edu

Support

Funding was provided by the National Institute of Health, F32NS074839 and K99/R00NS085035 to A.C.M, R01MH109498 to MG, R01EY012857 to J.O., and R01HD076585 and R21NS076950 to C.B.M.

We declare that we have no competing interests.

Abstract

Neural network function is based upon the patterns and types of connections made between neurons. Neuronal synapses are adhesions specialized for communication and they come in two types, chemical and electrical. Communication at chemical synapses occurs via neurotransmitter release whereas electrical synapses utilize gap junctions for direct ionic and metabolic coupling. Electrical synapses are often viewed as symmetrical structures, with the same components making both sides of the gap junction. By contrast, we show that a broad set of electrical synapses in zebrafish, *Danio rerio*, require two gap-junction-forming Connexins for formation and function. We find that one Connexin functions presynaptically while the other functions postsynaptically in forming the channels. We also show that these synapses are required for the speed and coordination of escape responses. Our data identify a genetic basis for molecular asymmetry at vertebrate electrical synapses and show they are required for appropriate behavioral performance.

Introduction

Brain function is derived from the connectivity patterns and types of synapses made between neurons within a circuit. Synapses come in two main types, chemical and electrical, that together dynamically define neural circuit function across all life stages and animal phyla (Connors & Long 2004; Meier & Dermietzel 2006; Pereda 2014). Chemical synapses are broadly used within the nervous system and are overtly asymmetric at the molecular and functional level, with communication between neurons achieved via presynaptic neurotransmitter release and postsynaptic neurotransmitter reception. Electrical synapses are best known for their roles in early nervous system development, however they are found throughout the brain from inception to adulthood and contribute to function from sensation to central processing to motor output (Hormuzdi et al. 2004). Electrical synapses are generally viewed as molecularly and functionally symmetric, allowing for very fast bidirectional ionic and metabolic neuronal communication (Connors & Long 2004). This direct route of communication is achieved by neuronal gap junctions (GJs) that are formed from plaques of tens to thousands of channels between the neurons (Raviola & Gilula 1973; Hormuzdi et al. 2004). While often viewed as simple channels, work in invertebrates has found that unique GJ-forming proteins can be contributed asymmetrically from each side of the synapse (Phelan et al. 2008; Starich et al. 2009). Moreover, the molecular asymmetry can create functional asymmetry (rectification) in ionic flow through the GJ (Phelan et al. 2008). In vertebrate nervous systems electron microscopy and electrophysiology suggests that electrical synapse structure and function can also be asymmetric (Brightman & Reese 1969; Rash et al. 2013). However, the genetic basis for such molecular asymmetry at vertebrate electrical synapses has never been identified.

Neuronal GJs are intercellular channels that directly connect two cytoplasms together allowing ions and molecules less than ~1 kilodalton to traverse between cells. They are composed of two hemi-channels, one contributed by each neuron, that interact via their extracellular domains to form the channel (Fig. 1A) (Connors & Long 2004). Vertebrate GJ-forming proteins are the Connexins (Cx) while invertebrates use an evolutionarily distinct but functionally equivalent set of Innexins (Phelan 2005). In mammals there are 21 genes encoding Cx proteins of which five are known to be expressed in neurons and to form electrical synapses (Connors & Long 2004; Söhl et al. 2005). A partial genome duplication that occurred in teleost fish has increased the number of Cx-encoding

genes, and the ensuing evolutionary trajectories saw some genes being duplicated, while others were lost (Eastman et al. 2006; Cruciani & Mikalsen 2007; Zoidl et al. 2008). Often individual cells or apposed cells express multiple different GJ-forming proteins providing the opportunity for heteromeric hemichannels made from multiple Cxs or heterotypic channels made by pairing hemichannels between cells with different Cxs (Palacios-Prado et al. 2014). In vertebrates, heterotypic GJs between cells in non-neuronal tissue are common (Goodenough & Paul 2009), however it has been notoriously difficult to identify heterotypic Cx configurations at electrical synapses in neurons.

Here we identify two Cxs used asymmetrically for the formation and function of electrical synapses in zebrafish. We focus on the Mauthner neural circuit, which mediates a fast escape behavior, since it has uniquely identifiable pre- and postsynaptic neurons making stereotyped electrical synapses that contribute to the escape response. We find that two Cx-encoding genes, *gjd1a/cx34.1* and *gjd2a/cx35.5*, are required for synapse assembly and function. Both of these Cx proteins are localized to synapses throughout the Mauthner circuit, as well as other synapses within the hindbrain and spinal cord, and each requires the other for recruitment to the synapse. Using chimeric analysis we demonstrate a dramatic asymmetry at electrical synapses in the circuit: *gjd1a/cx34.1* is necessary and sufficient postsynaptically while *gjd2a/cx35.5* is necessary and sufficient presynaptically for formation. Using high throughput behavioral analysis we find that the electrical synapses contribute to the speed and coordination of the Mauthner-induced escape response. Together our data support a model wherein molecularly asymmetric electrical synapses act in concert with chemical synapses to impart performance onto the neural network output.

Results

The *disconnect3* mutation disrupts *gjd1a/cx34.1* and electrical synapse formation

To investigate genes required for electrical synapse formation *in vivo* we used the Mauthner (M) neural circuit of larval zebrafish (Fig. 1B). The Mauthner circuit coordinates an escape response to a variety of threatening stimuli and produces the fastest sensorimotor reflex performed by fish (~5 milliseconds (ms) to initiate, ~10 ms to complete) (Eaton et al. 1977; Fetcho 1991; Burgess & Granato 2007; Satou et al. 2009). The Mauthner circuit that produces the escape is a combination of electrical, excitatory chemical, and inhibitory chemical synapses contained within a relatively

simple set of neurons that must be coordinated to ensure fast and robust escapes (Fetcho 1991). Key to the circuit's function is making unidirectional turns away from the stimulus. To do so, vibrational stimuli are transmitted via the VIIIth cranial nerve auditory afferents making prominent and stereotyped mixed electrical and glutamatergic chemical synapses at so-called Club Ending synapses that we refer to throughout as the Aud/M synapse (Pereda et al. 2004; Yao et al. 2014). Mauthner in turn sends a contralateral projection down the length of the spinal cord where it activates primary motorneurons (MNs) in each hemisegment, thereby producing the stereotypical C-bend-shaped escape away from stimulus (Fetcho 1991). The projecting Mauthner axon concurrently activates CoLo interneurons in each segment via excitatory electrical synapses; CoLo in turn re-crosses the spinal cord and inhibits MNs on the stimulus side, thereby ensuring coordinated turns away from stimulus (Satou et al. 2009). Throughout the paper we use the terms pre- and postsynaptic for electrical synapses based on three main criteria: 1) information flow, as described above, from auditory afferents (pre) to Mauthner dendrite (post), then from Mauthner axon (pre) to CoLo (post)(Fetcho 1991; Satou et al. 2009); 2) Mauthner itself is a bipolar neuron with unique axonal (pre) and dendritic (post) compartments (Kimmel et al. 1981); 3) both the Aud/M and M/CoLo electrical synapses have closely associated chemical synapse components with the neurotransmitter receptors localizing to postsynaptic compartments of the neurons (Mauthner dendrite in the hindbrain (Yao et al. 2014), CoLo proximal portion of the neurite on the ipsilateral side of the spinal cord (Miller et al. 2015)). The Mauthner and CoLo neurons can be visualized using the transgenic line *zf206Et(Tol-056)*, hereafter called *M/CoLo:GFP*, which expresses GFP in both neuron types (Satou et al. 2009). The electrical synapses of the Mauthner circuit can be visualized by immunostaining using a polyclonal antibody against the human Cx36 protein (Fig. 1C)(Miller et al. 2015).

To identify genes required for electrical synapse formation we mutagenized animals with N-ethyl-N-nitrosourea (ENU) to generate random genomic mutations and created gynogenetic-diploid mutant animals (Walker et al. 2009) to screen for disruptions to the Cx36 staining found at M/CoLo synapses at 3 days post fertilization (dpf)(Miller et al. 2015). We identified a mutation we called *disconnect3* (*dis3*) that caused a complete loss of Cx36 staining at the M/CoLo synapses (Fig. 1D and figure-associated table). Cx36 staining was disrupted at Mauthner electrical synapses, and other electrical synapses (see below) in *dis3* mutants across all timepoints examined (2 to 14 dpf).

dis3 mutants display normal numbers of Mauthner and CoLo neurons and their neurites contact one another in the spinal cord similar to wildtype (Fig. 1C,D). Moreover, *dis3* mutants display no gross morphological defects in nervous system morphology and neuronal number, have no defects in general body plan development, have normal developmental timing, are homozygous viable, and crosses between homozygous mutant animals produce viable offspring. We conclude that the gene disrupted by the *dis3* mutation has a broad but specific role in electrical synapse formation.

To identify the causative gene we used an RNA sequencing (RNA-seq)-based approach that identifies shared regions of genomic homozygosity in a pool of mutant animals (Miller et al. 2013). We separately pooled 108 mutant (*-/-*) and 108 wildtype (*+/+* and *+/-*) siblings and extracted and sequenced mRNA (Illumina Hi-Seq) from each pool. The sequences were aligned to the genome and single nucleotide polymorphisms (SNPs) were identified in the wildtype pool to serve as mapping markers. The SNP frequency was assessed in the mutant pool, identifying an ~1.8 megabase (Mb) region of homozygosity on chromosome 5 in *dis3* mutants (Fig. 1E). Within this region we used the RNA-seq data to look for potentially deleterious mutations and found that there were two missense changes to a Cx-encoding gene (Fig. 1F). Cx proteins are labeled for their molecular weight, while the genes encoding the proteins are named for one of five classes in which they reside (Söhl & Willecke 2004). The missense changes identified in *dis3* mutants disrupts the gene *gap junction delta 1a* (*gjd1a*) encoding a Cx with a predicated molecular weight of 34.1 kiloDaltons (Cx34.1). This gene is highly related to the mammalian *gjd2* gene encoding Cx36 (see below). For clarity throughout, when referring to zebrafish Cxs we will use both the official gene name as well as its molecular weight designation, in this case *gjd1a/cx34.1*. Within the *~1.8* Mb region of mapping there were an additional 10 missense mutations in other genes and 1 gene with significantly reduced expression compared to wildtype. To determine if the mutations in *gjd1a/cx34.1* were causative for the phenotype we generated an 8 base pair (bp) frame-shifting mutation at nucleotide 4 of exon 1 (*gjd1a*^{fh436}) using transcription activator-like-effector nucleases (TALENs) (Sanjana et al. 2012; Shah et al. 2015). We found that larvae homozygous for the frameshift mutation (*gjd1a*$^{fh436/fh436}$) phenocopy the loss of Cx36-staining at M/CoLo synapses observed in the *dis3* mutants; moreover, *gjd1a*^{fh436} failed to complement the *dis3* mutation (Fig. 1G and figure-associated table). We renamed the *dis3* mutation *gjd1a*^{fh360} and conclude that *gjd1a/cx34.1* is required for Mauthner electrical synapse formation.

gjd1 (Cx34) and *gjd2* (Cx35/Cx36) are part of a family of highly conserved genes/proteins

In mammals there are five unique Connexins that form electrical synapses, with the *gjd2/cx36* gene being the most studied due to its widespread use in the nervous system (Connors & Long 2004; Söhl et al. 2005; Pereda 2014). Previous work in zebrafish and goldfish has implicated two Cx36-related proteins, Cx34.7 and Cx35.1, as being present at electrical synapses (Pereda et al. 2003; O'Brien et al. 2004; Carlisle & Ribera 2014; John E. Rash et al. 2013). We wondered how *gjd1a/cx34.1* related to these and other Connexins and so used its sequence to search the zebrafish genome for similar genes. This identified three highly-related loci, two of these being the previously identified *gjd1b/cx34.7* and *gjd2b/cx35.1*, while the third is predicted to encode a Cx with a molecular weight of 35.5 kD, *gjd2a/cx35.5* (Fig. 2 and figure-associated table). Within this group of four Cx-encoding genes, all of the predicted proteins share greater than 85% amino acid identity to each other and to mammalian Cx36 proteins (Fig. 2A). The main variation in protein sequence arises in the intracellular loop, with some modest variation in the C-terminal tail (Fig. 2A,B). We examined the evolutionary relationship between these proteins and found that they represent two distinct Cx sub-families (Fig. 2C). In basal vertebrates (lamprey) we found only one gene within the family, this gene was subsequently duplicated creating two sub-families – the Cx35/36 proteins encoded by *gjd2* genes and the Cx34 proteins encoded by genes we have named *gjd1*. Genes within both of these families are found in lineages up to and including birds, but in mammals the *gjd1* family has apparently been lost. In bony fishes, including zebrafish, these gene families underwent another duplication event (Postlethwait et al. 2004), resulting in the four extant genes (Fig. 2C). Previous work has found that the *gjd1b/cx34.7* and *gjd2b/cx35.1* genes are expressed in the nervous system of zebrafish, analogous to *gjd2* (Cx36) expression in mammals (Li et al. 2009; Carlisle & Ribera 2014). We examined published RNA-seq and EST datasets (*Ensembl*: WTSI stranded RNA-Seq, WTSI, KIT, Yale (Yates et al. 2016) and the UCSC Genome Browser (Kent et al. 2002)) and found that all four of the *gjd1* and *gjd2* genes in zebrafish are enriched for nervous system expression while being reduced or absent from other tissues. Together it appears that all of the *gjd1/2* genes have the potential to play broad roles in neural circuit formation and function.

gjd1a/cx34.1 and *gjd2a/cx35.5* are required for electrical synapse formation and function

While we identified *gjd1a/cx34.1* as being required for M/CoLo synapse formation (Fig. 1) we wondered if any of the other closely related genes were required for Mauthner circuit synaptogenesis. To examine these genes we generated mutations in each of them (Fig. 2B) and analyzed the effect of their loss on electrical synapse formation (Shah et al. 2015). We examined the electrical synapses made onto the M cell body and dendrite (Fig. 3A) and particularly focused on the stereotyped Aud/M synapses (Fig. 3A arrows, 3B) and the M/CoLo electrical synapses of the spinal cord (Fig. 3C). The anti-human-Cx36 antibody used for staining recognizes all four of the proteins generated by the zebrafish *gjd1/2* genes when each is expressed in HeLa cells (see Methods). We found that *gjd1a/cx34.1* mutants affected not only the M/CoLo synapses in the spinal cord, but also the Aud/M synapses, as well as other electrical synapses made onto the Mauthner cell body (Fig. 3D-F). In analyzing mutants for the other three genes, we found that *gjd2a/cx35.5* mutants also lost Mauthner electrical synapses in the hindbrain and spinal cord (Fig. 3G-I) while *gjd1b/cx34.7* and *gjd2b/cx35.1* had no effect on Cx36 staining (Fig. 3J,K). In quantifying the amount of Cx36-staining at Mauthner synapses we found that the loss of *gjd2a/cx35.5* resulted in a complete absence of detectable Cx protein at synapses throughout the Mauthner circuit. In *gjd1a/cx34.1* mutants the Cx36 staining at M/CoLo synapses was lost, but we note that there was ~4 fold reduction in the amount of staining at the Aud/M synapses (Fig. 3E,J,K). This residual staining was not eliminated in double or triple mutants between *gjd1a* and *gjd1b or gjd2b* (Fig. 3L). On the whole we conclude that the gap junctions that form the Mauthner circuit electrical synapses require both *gjd1a/cx34.1* and *gjd2a/cx35.5* for their formation.

To investigate whether Cx34.1 and Cx35.5 were required for electrical synapse function we examined whether the passage of the gap junction permeable dye neurobiotin (Nb) was impaired in mutants. We retrogradely labeled Mauthner axons with Nb from caudal spinal cord transections (Fig. 4A) and then detected Nb within the CoLo cell bodies in the *M/CoLo:GFP* line (Fig. 4B) (Miller et al. 2015). In both *gjd1a/cx34.1* and *gjd2a/cx35.5* mutants we found that no Nb was transferred from Mauthner to CoLo (Fig. 4B,D,F). That Nb passage is completely blocked in both mutants supports the idea that Mauthner circuit electrical synapses are dependent on both Cx34.1 and Cx35.5 for their function. Taken together these data suggest that there is an intimate interaction between these two Cxs required for the establishment of M electrical synapses.

gjd1a (Cx34.1) and *gjd2a* (Cx35.5) are localized at and required for the majority of electrical synapses in the hindbrain and spinal cord

To examine whether Cx34.1 and Cx35.5 are both present at electrical synapses we generated antibodies that specifically recognized either protein (see Methods for details). Both antibodies generated staining patterns highlighting the same structures in the hindbrain and spinal cord as staining with the antibody against human Cx36 (Fig. 5A and figure-associated table). Cx34.1 and Cx35.5 staining overlapped nearly completely, but there were rare examples where staining was apparent for only one of the two Cx proteins. At Mauthner circuit electrical synapses Cx34.1 and Cx35.5 staining was completely overlapping at the individually identifiable Aud/M and M/CoLo synapses in the hindbrain and the spinal cord (Fig. 5A-C). In *gjd1a/cx34.1* mutants we found that Cx34.1 staining was lost while in the *gjd2a/cx35.5* mutants we found that Cx35.5 staining was lost supporting both the specificity of the antibodies as well as the deleterious nature of the mutations (Fig. 5D-I). In *gjd2a/cx35.5* mutants we found that Cx34.1 staining was lost from Aud/M and M/CoLo synapses suggesting Cx34.1 requires Cx35.5 for its localization (Fig. 5G-I). In *gjd1a/cx34.1* mutants we found that Cx35.5 was completely lost from M/CoLo synapses (Fig. 5F) and residual Cx35.5 staining was found at Aud/M synapses similar to what was observed with the human Cx36 antibody (Fig. 5D,E, Fig. 3D,E,J,K). Thus Cx35.5 also requires Cx34.1 for its localization. The residual staining in *gjd1a/cx34.1* mutants at Aud/M synapses suggests that Cx35.5 may form a subset of gap junctions with either itself or an as yet unidentified Cx that supports its localization and detection. Additionally, in both *gjd2a/cx35.5* and *gjd1a/cx34.1* mutants we detected dim Cx34.1 and Cx35.5-positive puncta, respectively, that were not associated with the Mauthner circuit (Fig. 5D-I). Such staining may represent synapses at which Cx34.1 and Cx35.5 do not require one another for their localization and stabilization. Altogether our results suggest that both Cx34.1 and Cx35.5 are broadly expressed and used throughout the hindbrain and spinal cord of zebrafish. Moreover, where Cx34.1 and Cx35.5 are found colocalized each requires the other to be stabilized and detectable at the electrical synapses.

Mauthner circuit electrical synapses require *gjd1a/cx34.1* in postsynaptic neurons and *gjd2a/cx35.5* in presynaptic neurons

Since we found that (*gjd1a*) Cx34.1 and (*gjd2a*) Cx35.5 are colocalized and required for one another's localization at Mauthner synapses we wondered where the two Cxs were required for

electrical synapse assembly. Given that electrical synapses are composed from Cx hemichannels contributed by apposing neurons (Fig. 1A), both Cx34.1 and Cx35.5 could be found on both sides of the synapse (heteromeric hemichannels), or instead each could be found exclusively on one side or the other (heterotypic channels), generating an asymmetric synapse. To test where each gene was required for electrical synapse formation we performed cell transplants at the blastula stage (Kemp et al. 2009) to create chimaeric animals containing wildtype and mutant cells and examined in which neuron of the circuit (auditory, Mauthner, or CoLo) the genes were required. We focused on the Mauthner circuit because we are able to associate the stereotyped synapses of the circuit with the uniquely identifiable pre- and postsynaptic neurons (see Fig. 1B and associated discussion). To create chimaeric animals we transplanted cells at the blastula stage from donor embryos marked with either the *M/CoLo:GFP* transgene or Biotin Dextran (BD) into host embryos lacking the same marker and examined the resulting embryos at 5 dpf (Fig. 6). To mark the presynaptic auditory afferent neurons and examine the hindbrain Aud/M synapses we transplanted cells from non-transgenic, BD-injected embryos into an *M/CoLo:GFP* host. To mark the postsynaptic Mauthner neurons in experiments examining the Aud/M synapse, and in all experiments in the spinal cord examining M/CoLo synapses, we transplanted cells from *M/CoLo:GFP* transgenic donors into a non-transgenic host. Such chimaeric animals allowed us to unambiguously identify from which embryo the neurons of the Mauthner circuit were derived based on the presence or absence of the markers used in each experiment.

In control chimeras with donor-derived presynaptic or postsynaptic neurons we saw no effect on Cx36 staining at Aud/M or M/CoLo synapses (Fig. 6A-E). Similarly, when presynaptic neurons (auditory afferent neurons in the hindbrain (Fig. 6F) or Mauthner in the spinal cord (Fig. 6I)) lacked *gjd1a/cx34.1* the electrical synapses were normal. However, when the postsynaptic neuron (Mauthner in the hindbrain (Fig. 6G,H) or CoLo in the spinal cord (Fig. 6J)) lacked *gjd1a/cx34.1* the electrical synapses were affected. Conversely, we found exactly the opposite requirement for *gjd2a/cx35.5:* removing its function presynaptically, but not postsynaptically, resulted in the loss of associated electrical synapses (Fig. 6K-O). Moreover, presynaptic removal of g*jd2a/cx35.5* reveals a complete loss of Cx36-staining at any associated synapse, while postsynaptic loss of *gjd1a/cx34.1* resulted in no staining at M/CoLo synapses and an ~4 fold reduction of Cx36 staining at Aud/M synapses (Fig. 6P,Q), consistent with the decrease observed in whole mutant animals

(Fig. 3J,K). This suggests that Cx35.5 and Cx34.1 are the exclusive pre- and postsynaptic Cxs, respectively, at M/CoLo synapses (Fig. 6Q). At the Aud/M synapses, Cx35.5 is the sole presynaptic Cx while Cx34.1 is required postsynaptically for the majority of GJ channels (Fig. 6P). The remaining Cx36-staining at Aud/M synapses when *gjd1a/cx34.1* is removed postsynaptically suggests some other Cx is stabilizing presynaptic Cx35.5; however removal of *gjd2a/cx35.5* postsynaptically does not affect Aud/M Cx36 staining (Fig. 6P) suggesting an unknown Cx may contribute to the synapse. We note that even within the single Mauthner neuron both Cx-encoding genes are required for electrical synapse formation, but their functions are spatially restricted to the dendrite (*gjd1a/cx34.1* , Fig. 6G,H) versus the axon (*gjd2a/cx35.5* , Fig. 6N). We conclude that *gjd2a/cx35.5* and *gjd1a/cx34.1* are required exclusively pre- and postsynaptically, respectively, to create Mauthner circuit electrical synapses.

The above transplant experiments suggest that Mauthner electrical synapses are heterotypic, with unique Cxs used on each side of the synapse. Moreover, our results suggest that trans-synaptic interaction between the Cxs is required for stabilization, and thereby detection via antibody staining, at the Mauthner synapses. This would help explain why when we remove either *gjd2a/cx35.5* or *gjd1a/cx34.1* we observe no staining of the other Cx at the synapse. This model predicts that in a *gjd2a/Cx35.5* mutants the postsynaptic Cx34.1 should still be available to make electrical synapses if provided with an appropriate presynaptic Cx (and vice versa). To test this notion and ask if Cx35.5 or Cx34.1 are sufficient pre- and postsynaptically, respectively, we created chimeric animals as above except we transplanted from wildtype *M/CoLo:GFP* embryos into a non-transgenic mutant hosts (Fig. 7). We found that when the postsynaptic neuron was wildtype in a *gjd1a/cx34.1* mutant the electrical synapses were rescued (Fig. 7A,B,D); however, when the presynaptic neuron was wildtype there was no rescue (Fig. 7C). Conversely, a wildtype presynaptic neuron was sufficient to rescue the synapse in a *gjd2a/cx35.5* mutant (Fig. 7G), but had no effect when the wildtype neuron was postsynaptic (Fig. 7E,F,H). In other words, Cx35.5 is sufficient to rescue the synapse if it is present in the presynaptic neurons while Cx34.1 is sufficient to rescue the synapse if it is present in the postsynaptic neuron. We note that the fold-rescue of Cx36 staining by a wildtype postsynaptic neuron was greater at M/CoLo as compared to Aud/M synapse (Fig. 7I,J); this ~4 fold rescue is consistent with the fold reduction seen in *gjd1a* mutants and postsynaptic loss of *gjd1a* at these same synapses (see Fig. 3J,K and Fig. 6P,Q). Altogether

we conclude that electrical synapse formation in the Mauthner circuit requires presynaptic Cx35.5 and postsynaptic Cx34.1 and that each Cx is required for the localization of the other via an interaction with the appropriate Cx in an adjacent cell.

Electrical synapses are required for speed and coordination of the Mauthner-induced escape response

To test how electrical synapses contributed to the escape response we examined the behavior of mutant and wildtype siblings using high-throughput behavioral analysis in free-swimming 6 dpf larvae (Wolman et al. 2015). The Mauthner circuit generates a fast escape response away from threatening stimuli using a combination of both electrical and chemical synapses (Fetcho 1991); for an explanation of Mauthner circuit function see Fig. 1B and associated discussion above. At 6 dpf there are approximately six auditory afferent neurons making mixed electrical/glutamatergic chemical synapses onto Mauthner (Aud/M); the electrical component of the postsynaptic response occurs 1-3 ms after afferent stimulation and happens just prior to that of its glutamatergic counterpart (Yao et al. 2014). By contrast, electrophysiology at the M/CoLo synapse suggests a single, excitatory electrical coupling allowing Mauthner to activate CoLo during an escape (Satou et al. 2009). Thus, electrical synapses are suggested to have unique effects on the initiation (Aud/M) and coordination (M/CoLo) of the Mauthner-induced escape response.

To test mutant behavior animals were placed into individual chambers in a multi-well testing stage illuminated by infrared light and were subjected to startling vibrational (acoustic) stimuli while being monitored with a high speed camera to capture the kinematics, or body movements, of escape responses. Each animal and its behavioral response was analyzed using FLOTE software (Burgess & Granato 2007), which automatically tracks movement parameters of the larvae. FLOTE can distinguish between Mauthner-induced short latency C-bend (SLC) escape responses and the longer latency escapes generated by related but distinct circuits (Burgess & Granato 2008). We analyzed the kinematics of the 6 dpf larval escape response from crosses between heterozygous animals (incross of *gjd1a/cx34.1*$^{+/-}$ *or gjd2a/cx35.5*$^{+/-}$*)*. Behavioral testing and analysis was performed blind followed by genotyping of each larva and comparisons of responses between wildtype siblings and mutants. We found that mutants produced SLCs at similar frequencies compared to their wildtype siblings (Fig. 8A, note that we found no difference between wildtype

siblings from the *gjd1a/cx34.1*$^{+/-}$ *or gjd2a/cx35.5*$^{+/-}$ crosses and so have collapsed these two groups into a single wt data point in Fig. 8; individual statistics can be found in the figure-associated table and lead to the same conclusions). However, we found that both *gjd1a/cx34.1* and *gjd2a/cx35.5* mutants initiated escape responses ~2ms (40%) slower than their wildtype siblings (Fig. 8B). In these 'long-latency' SLC responses the kinematics of the escape often had normal turn angles, maximum angular velocity, and other parameters known to be associated with Mauthner induced escapes, albeit happening later than in wildtype (Fig. 8C-H). However, a subset of mutant responses (~20% in each genotype) occurred with an abnormally shallow maximum angle of the C-bend (Fig. 8C, arrow) as well as abnormally slow maximum angular velocities (Fig. 8D, arrow). These abnormal responses suggested a defect in performing the stereotyped C-bend shape of the escape response and so we reanalyzed the video data from these events and found that both *gjd1a/cx34.1* and *gjd2a/cx35.5* mutants often produced abnormal postural responses to the auditory startle stimuli (Fig. 8I-L). We found that as these animals initiated movements they displayed only slight bends to one side, creating "kinked" or "S-shaped" postures, and also shortening their body axis. These animals would stay in this state for 4-10 ms then produce a secondary movement in the opposite direction of the initial, small head movement, followed most often by swimming behavior. These secondary movements were likely the normal counter bend and swimming motions that occur after a Mauthner induced escape (Burgess & Granato 2008; Satou et al. 2009), but in these cases they occurred after a failed escape. From these data we conclude that electrical synapses contribute to the speed and coordination of the Mauthner induced escape response.

Discussion

Our genetic analysis in the zebrafish Mauthner circuit strongly support a model where these vertebrate electrical synapses are molecularly asymmetric with unique pre- and postsynaptic Cxs making the neuronal GJ channels (Fig. 9A). One intriguing possibility is that differences in the pre- and postsynaptic Cxs would bias the passage of ionic flow through the GJ creating a “rectified” electrical connection (Palacios-Prado et al. 2014). Indeed such is the case for two Innexins, Shaking-B(Neural+16) and Shaking-B(lethal), that in *Drosophila* form a molecularly asymmetric synapse; when these hemi-channels are paired in apposing *Xenopus* oocytes they allow for biased current flow (Phelan et al. 2008). In adult goldfish freeze-fracture immunolabeling and electron microscopy (EM) suggested that the club ending synapses of Mauthner were molecularly asymmetric (see below for discussion of Cx usage) and electrophysiology found that ionic flow was preferentially directed from the post- to presynaptic terminal; the authors suggested that this functional asymmetry leads to cooperativity amongst the multiple converging auditory afferent axons thereby promoting the Mauthner escape response (Rash et al. 2013). Whether the configuration we find here of presynaptic Cx35.5 paired with postsynaptic Cx34.1 is sufficient to produce biased current flow across the channel is unclear; however the Cx asymmetry may not act alone in biasing synaptic function. Cx function can be modified by differences in the intracellular milieu such as Mg++ concentration (Palacios-Prado et al. 2014) and differential phosphorylation (Pereda 2014) or perhaps different pre- and postsynaptic protein interactions may bias function. The molecular asymmetry of Cxs we identify suggests that GJ-associated proteins may also be asymmetrically distributed. Intriguingly, we previously found that the autism associated gene *neurobeachin*, which encodes a scaffolding protein thought to act within the trans-Golgi network, was required postsynaptically for electrical synaptogenesis (Miller et al. 2015). Ultimately, such asymmetric neuronal gap junctions are likely to occur in situations where electrical synapses are made between unique compartments, such as axonal-to-cell-body or axonal-to-dendritic configurations, as each Cx may traffic, localize, or be required separately in different compartments. Future work is sure to extend the idea of molecular and functional asymmetry of electrical synapses and they are likely to be important for the development, function, and plasticity of neural circuits.

In our experiments we found that *gjd1a/cx34.1* and *gjd2a/cx35.5* create the electrical synapses of the Mauthner circuit as well as many other synapses of zebrafish. As mentioned above, EM in goldfish has instead suggested that Cx35.1 and Cx34.7 may create the Aud/M synapses, yet we find that the genes encoding these two Cxs are not required in zebrafish (Fig. 3). What accounts for this discrepancy? First, it is likely that the goldfish and zebrafish Aud/M synapses are constructed with the same Cxs, but this need not be the case and could account for differences. Moreover, the goldfish synapses were examined at adulthood while our work was in larval stages; it is conceivable that these electrical synapses could change their composition during development and maturation. Second, we have found that the antibodies used in the previous study label all zebrafish Mauthner circuit electrical synapses at larval stages (data not shown). This, when put in the context of our genetic evidence for the requirement for *gjd1a/cx34.1* postsynaptically and *gjd2a/cx35.5* presynaptically, suggests that these previously used antibodies cross react with Cx34.1 and Cx35.5. The most parsimonious scenario would be that the Cx35.1 antibody cross reacts with Cx35.5, while the Cx34.7 antibody cross reacts with Cx34.1, making for a consistent picture between the genetics we present here and the previous freeze-fracture immuno-EM data (Rash et al. 2013). Together, these data strongly support a model wherein the Aud/M synapses are molecularly asymmetric. We also find that there may be an “unidentified” Cx at the Aud/M electrical synapses that is required for a subset of the gap junction channels (Fig. 3E,5E,6H). Alternatively the residual staining we observe may be due to compensation in *gjd1a/cx34.1* mutants and/or to *gjd2a/*Cx35.5 trafficking to postsynaptic sites at some relatively low rate; future work using freeze-fracture EM in mutants will shed light on this issue. Regardless, it is intriguing to speculate that the Aud/M electrical synapses may contain complexity beyond the asymmetry we have focused on here. Our genetic and chimaeric evidence also support Cx molecular asymmetry at M/CoLo synapses in the spinal cord. This configuration is likely used frequently given the broad colocalization of Cx34.1 and Cx35.5 and their co-requirement for localization (Fig. 5). Molecular asymmetries at electrical synapses are not confined to fish, but are found broadly throughout the nervous systems of *C. elegans* (Starich et al. 2009), medicinal leech (Kandarian et al. 2012), *D. melanogaster* (Curtin et al. 1999; Phelan et al. 2008), crab (Shruti et al. 2014), and there have been suggestions, though no definitive proof, that such may occur in mammals as well (Cha et al. 2012; Haas et al. 2011; Zolnik & Connors 2016). If such does occur in mammalian systems it would have to rely on a different set of Cxs than in zebrafish as mammals appear to have lost the

gjd1/cx34 family of genes, leaving only the single, related *gjd2/cx36* gene (Fig. 2). However, there are four other Cxs known to make electrical synapses in mammals (Connors & Long 2004; Söhl et al. 2005; Pereda 2014), and the extent of their use and the configurations of GJs they create is poorly understood. We expect that molecularly asymmetric electrical synapses are likely to be a part of all nervous systems given that they underlie important functional effects on the properties of neural circuit computation (Phelan et al. 2008; Rash et al. 2013).

How do the electrical synapses contribute to neural circuit computation and behavioral output? We found that the *cx* mutants are slower to respond to vibrational stimuli, but can still produce fast escape responses consistent with Mauthner activation. This increased latency is most likely attributable to defects at the Aud/M mixed electrical/chemical synapses (Fig. 9B). While we cannot rule out the possibility that electrical synapses upstream of Mauthner are required for the observed defects, or that the loss of electrical synapses somehow effects chemical synapses within the Mauthner circuit, we prefer the model that the reduction in response speed is due to the loss of the electrical component of the Aud/M synapses given that these synapses are required for Mauthner activation and sufficient to create the fast escape response (O'Malley et al. 1996). This idea is supported by electrophysiological recordings of Aud/M synapses in wildtype larval zebrafish at stages similar to those we analyzed where the electrical response occurs ~2 milliseconds faster than that of the chemical synaptic response (Yao et al. 2014). We also observed that a subset of escape responses in *cx* mutants display coordination defects. This is likely due to the loss of the M/CoLo synapses in the spinal cord as similar behavioral defects have been observed when CoLos are laser ablated or when strychnine is used to block inhibitory synapses (Satou et al. 2009; Marsden & Granato 2015). These uncoordinated responses likely only occur in a subset of escapes because the CoLos are productively engaged in the behavioral output only in cases where both Mauthner neurons fire in response to the stimulus. In wildtype when both Mauthners fire turning is unidirectional; this is achieved by the first-activated Mauthner's action potential exciting CoLos, which then recross the spinal cord to the 'late-activated Mauthner side' and inhibit the motor neurons before the late-activated Mauthner's action potential arrives – this ensures a unidirectional turn (see Fig. 9B for circuit diagram)(Fetcho 1991; Satou et al. 2009). When calcium activity of Mauthner is monitored in experimental paradigms similar to those we used it was found that both Mauthner neurons were activated at rates in line with the behavioral defects we observe

(Satou et al. 2009; Marsden & Granato 2015). Thus it is likely that the coordination defects we observe in mutants are due to the loss of the M/CoLo synapses. We have not observed other overt defects in behavior in our mutants, in line with a lack of overt behavioral defects in mice mutant for *gjd2/cx36* (Güldenagel et al. 2001; De Zeeuw et al. 2003; Jacobson et al. 2010; Zlomuzica et al. 2012). However, given the breadth of Cx34.1/Cx35.5 staining we expect these electrical synapses to contribute to many circuit computations and behaviors of the animal. As circuit and behavioral analysis becomes more sophisticated we expect to identify broad contributions of the Cx34.1/Cx35.5 electrical synapses, and Cx36 synapses in mammals as well, to behavior, memory, and plasticity of the nervous system.

Methods

Fish, lines, and maintenance

All animals were raised in an Institutional Animal Care and Use Committee (IACUC)-approved facility at the Fred Hutchinson Cancer Research Center. Zebrafish, *Danio rerio*, were bred and maintained as previously described (Kimmel et al. 1995). Rachel Garcia provided animal care and Dr. Rajesh K. Uthamanthil, DVM, provided veterinary care. *gjd1a*$^{fh360(dis3)}$ was isolated from an early-pressure, gynogenetic diploid screen (Walker et al. 2009) using ENU as a mutagen and animals were outcrossed from an *AB background into a Tuebingen background for mapping. *gjd1a*^{fh436}, *gjd1b*^{fh435}, *gjd2a*^{fh437}, and *gjd2b*^{fh454} were generated using TALENs (Neville E Sanjana et al. 2012) targeting the 1st exon. *gjd2b*^{fh329} was generated via TILLING (Kettleborough et al. 2011). See Fig. 2 and table-associated data for information on all alleles. Stable zebrafish lines carrying each mutation were Sanger sequenced to verify mutations. All were maintained in the *M/CoLo*:GFP (*Et*(*Tol-056:GFP*)) background (Satou et al. 2009), which is a *AB/Tu background.

RNA-seq-based mutant mapping

Larvae in the F3 generation were collected at 3 dpf from crosses of known *gjd1a*$^{fh360(dis3)}$ heterozygous animals, were anesthetized with MESAB (Sigma, A5040), and the posterior portion was removed and fixed for phenotypic analysis via immunohistochemistry (see below) while the anterior portion was placed in Trizol (Life Technologies, 15596-026), homogenized, and frozen to preserve RNA for sequencing. After phenotypic identification mutant (-/-) and wildtype sibling (+/+ and +/-) RNA was pooled separately from 108 embryos each. From each pool total RNA was extracted and cDNA libraries were created using standard Illumina TruSeq protocols. Each library was individually barcoded allowing for identification after multiplexed sequencing on an Illumina HiSeq 2000 machine. In brief, mapping was performed by identifying high quality “mapping” single nucleotide polymorphisms (SNPs) in the wildtype pool and assessing these positions in the mutant pool for their frequency. The average allele frequency in mutants, using a sliding-window of 50-neighboring loci, was plotted across the genome and linkage was identified as the region of highest average frequency. Within the linked region candidate mutations causing nonsense or missense changes, or those affecting gene expression levels, were identified as previously described (Miller et al. 2013). Details can be found at www.RNAmapper.org.

Cloning and characterization of Connexin genes

We used the *gjd1a/cx34.1* sequences to search the Zv10 genome of zebrafish for other genes with similar sequence. From these searches we identified four loci, *gjd1a/cx34.1* (chr5), *gjd1b/cx34.7* (chr15), *gjd2a/cx35.5* (chr17), and *gjd2b/cx35.1* (chr20), as the only locations with significant homology. All four are two-exon genes, however the gene encoding Cx35.5 is annotated on the zebrafish Zv10 genome as having the first exon downstream and in the opposite orientation of the second exon. This arrangement is most likely due to an inappropriately assembled region of the genome for three reasons: 1) we cloned a full-length transcript from a cDNA library using primers to the 5'- and 3'-UTRs, 2) the gene results in a protein product, 3) the gene results in a protein detectable by an antibody made against it (see results for points 2 and 3).

Antibody generation and validation

Antibodies were generated at the Fred Hutchinson Antibody Technology Facility (https://sharedresources.fredhutch.org/core-facilities/antibody-technology). We used the variable regions of the intracellular loop from *gjd1a/*Cx34.1 and *gjd2a/*Cx35.5 (Fig. 2A,B) to generate peptide antibodies to each protein and first tested the specificity of antibodies on each Cx protein individually expressed in HeLa cells. We found several antibodies against each Cx that specifically recognized only the intended target Cx and not the others and screened each of these using whole-mount immunohistochemistry of 5 dpf zebrafish larvae. We found that these antibodies generated staining patterns highlighting the same structures in the midbrain, hindbrain, and spinal cord as staining with the antibody against human Cx36 used above (Fig. 5 and associated data). The human anti-Cx36 antibody was also found to recognize all four zebrafish Cx36-related proteins (Fig. 5 and associated data). We did not detect staining in areas anterior of the midbrain, but we did not perform the sectioning required to recognize electrical synapses in the retina and other anterior regions (Li et al. 2009). In *gjd1a/cx34.1* mutants we found that staining for Cx34.1 protein was lost while in the *gjd2a/cx35.5* mutants we found that Cx35.5 protein staining was lost supporting both the specificity of the antibodies as well as the deleterious nature of the mutations (Fig. 5).

Immunohistochemistry

Anesthetized embryos from 2-14 dpf were fixed in either 2% trichloroacetic (TCA) acid for 3 hours

or 4% paraformaldehyde (PFA) for 1 hour. Fixed tissue was then washed in PBS + 0.5% TritonX100, followed by standard blocking and antibody incubations. Tissue was cleared step-wise in a 25%, 50%, 75% glycerol series and was dissected and mounted for imaging. Primary antibodies used were: chicken anti-GFP (abcam, ab13970, 1:250), rabbit anti-human-Cx36 (Invitrogen, 36-4600, 1:200), mouse anti-RMO44 (Life Technologies, 13- 0500, 1:100), and rabbit anti-Cx34.1 and mouse anti-Cx35.5 (1:100). All secondary antibodies were raised in goat (Life Technologies, conjugated with Alexa-405, -488, -555, -594, or -633 fluorophores, 1:250). Neurobiotin and Biotin Dextran were detected using fluorescently-tagged streptavidin (Life Technologies, conjugated with Alexa-633 fluorophores, 1:500).

Neurobiotin retrograde labeling

Anesthetized 5 dpf embryos were mounted in 1% agar and a caudal transsection through the dorsal half of the embryo was made with an insect pin at somite 20-25. A second insect pin loaded with 5% neurobiotin (Nb) solution was quickly applied to the incision. Animals were unmounted from the agar and allowed to rest for 3 hours while anesthetized to allow neurobiotin to pass from Mauthner into the CoLos. Animals were then fixed in 4% PFA for 2 hours and processed for immunohistochemistry. CoLo axons project posteriorly for a maximum of two segments; therefore measurements of Nb in CoLo were analyzed at least three segments away from the lesion site.

Cell transplantation

Cell transplantation was done using standard techniques at the blastula stage (Kemp et al. 2009). For “mutant into wildtype” experiments examining the spinal cord M/CoLo synapses and assessing the postsynaptic Mauthner of Aud/M synapses, animals heterozygous for a *cx* mutation and carrying the *M/CoLo:GFP* transgene were incrossed while hosts were non-transgenic AB; for “wildtype into mutant”, *M/CoLo:GFP* animals were incrossed while hosts were an incross of animals heterozygous for a *cx* mutation that were not transgenic. For assessing the presynaptic auditory afferent contribution to the Aud/M synapses embryos were injected with biotin-dextran at the 1-cell stage and later transplanted from appropriate genotypes. Approximately 20 cells were deposited 1-5 cell diameters away from the margin at the sphere/dome stage (4-4.5 hpf) with a single embryo donating to 3-5 hosts. Embryos were allowed to grow until 5 dpf at which point they were processed for immunostaining. Donor (mutant to wildtype) or host (wildtype to mutant)

embryos were genotyped.

Confocal imaging and analysis

All images were collected on a Zeiss LSM 700 confocal microscope using 405, 488, 555, and 639 laser lines, with each line's data being collected sequentially using standard pre-programmed filters for the appropriate Alexa dyes. All Z-stacks used 1uM steps. Images were processed and analyzed using Fiji (Schindelin et al. 2012) software. Within each experiment all animals were stained together with the same antibody mix, processed at the same time, and all confocal settings (gain, offset, objective, zoom) were identical. For quantitating fluorescent intensity, synapses were defined as the region of contact between the neurons of interest (Aud/M or M/CoLo). A standard region of interest (ROI) surrounding each synapse was drawn and the mean fluorescent intensity was measured across at least 4 uMs in the Z-direction with the highest value being recorded. For neurobiotin backfills fluorescent intensity was measured using a standard ROI encompassing the entire Mauthner or CoLo cell body. Statistics were computed using Prism software (GraphPad). Figure images were created using Fiji, Photoshop (Adobe) and Illustrator (Adobe). Colors for all figures were modified using the Fiji plugin Image5D.

Behavioral imaging and analysis

Behavioral experiments were performed on 6 dpf larvae as previously described (Burgess & Granato 2007; Wolman et al. 2011; Wolman et al. 2015). Briefly, larvae were placed in individual wells of a 16-well grid and exposed to 3 ms, 1000 Hz acoustico-vibrational stimuli delivered by an acoustic shaker at 26 dB. Stimulus intensities were calibrated with a PCB Piezotronics accelerometer (model #355B04). All animals received 10 stimuli separated by 20 sec, which is sufficient to ensure that no habituation occurs over the course of the experiment (Wolman et al. 2011). Movements were captured using a high-speed camera (RedLake MotionPro) at 1000 frames/sec, and movies were analyzed with the FLOTE software package as previously described (Burgess & Granato 2007). Short latency C-bend startle responses (SLCs) driven by Mauthner were measured and defined by the previously established kinematic parameters of initiation latency, turning angle, turn duration, and maximum angular velocity (Burgess & Granato 2007). After testing, larvae were transferred to 96-well plates and processed for subsequent genotyping.

Author Contributions

A.C.W. and A.C.M. performed the experiments for Figs. 1-7. K.M. and A.C.M. performed experiments for Fig. 8. A.C.W. and A.C.M quantified all data and generated images for publication. A.N.S. created the TALENs directed against *cx* genes and generated the mutant animals. A.C.M. and C.B.M. collaborated on the manuscript. All authors edited the manuscript.

Statement of Competing Interests

None.

Acknowledgements

We thank Rachel Garcia for superb animal care, Kathryn Helde for help with the forward genetic screen, Lila Solnica-Krezel for ENU-mutagenized male zebrafish, Shin-Ichi Higashijima for the *M/CoLo:GFP* line, and the Fred Hutchinson Cancer Research Center's Genomic Resource Center, particularly Jeff Delrow, Andy Marty, Alyssa Dawson, and Ryan Basom, for sequencing library preparation, sequencing, and help in data processing. Funding was provided by the National Institute of Health, F32NS074839 and K99/R00NS085035 to A.C.M, R01MH109498 to MG, R01EY012857 to J.O., and R01HD076585 and R21NS076950 to C.B.M.

References

Brightman, M.W. & Reese, T.S., 1969. Junctions between intimately apposed cell membranes in the vertebrate brain. *Journal of Cell Biology*, 40(3), pp.648–677.

Burgess, H.A. & Granato, M., 2007. Sensorimotor gating in larval zebrafish. *The Journal of neuroscience : the official journal of the Society for Neuroscience*, 27(18), pp.4984–94. Available at: http://www.ncbi.nlm.nih.gov/sites/entrez?Db=pubmed&DbFrom=pubmed&Cmd=Link&LinkName=pubmed_pubmed&LinkReadableName=Related Articles&IdsFromResult=17475807&ordinalpos=3&itool=EntrezSystem2.PEntrez.Pubmed.Pubmed_ResultsPanel.Pubmed_RVDocSum%5Cnhttp://www.jne.

Burgess, H.A. & Granato, M., 2008. The neurogenetic frontier--lessons from misbehaving zebrafish. *Briefings in Functional Genomics and Proteomics*, 7(6), pp.474–482. Available at:

http://bfgp.oxfordjournals.org/cgi/doi/10.1093/bfgp/eln039.

Carlisle, T.C. & Ribera, A.B., 2014. Connexin 35b expression in the spinal cord of Danio rerio embryos and larvae. *Journal of Comparative Neurology*, 522(4), pp.861–875.

Cha, J. et al., 2012. Variety of horizontal cell gap junctions in the rabbit retina. *Neuroscience Letters*, 510(2), pp.99–103.

Connors, B.W. & Long, M.A., 2004. Electrical Synapses in the Mammalian Brain. *Annual review of neuroscience*, 27(1), pp.393–418. Available at: http://www.ncbi.nlm.nih.gov/pubmed/15217338%5Cnhttp://arjournals.annualreviews.org/loi/neuro.

Cruciani, V. & Mikalsen, S.-O., 2007. Evolutionary selection pressure and family relationships among connexingenes. *Biological Chemistry*, 388(3), pp.253–264. Available at: http://www.reference-global.com/doi/abs/10.1515/BC.2007.028.

Curtin, K.D., Zhang, Z. & Wyman, R.J., 1999. Drosophila has several genes for gap junction proteins. *Gene*, 232(2), pp.191–201.

Eastman, S.D. et al., 2006. Phylogenetic analysis of three complete gap junction gene families reveals lineage-specific duplications and highly supported gene classes. *Genomics*, 87(2), pp.265–274. Available at: http://linkinghub.elsevier.com/retrieve/pii/S088875430500296X.

Eaton, R.C. et al., 1977. Functional development in the Mauthner cell system of embryos and larvae of the zebra fish. *Journal of neurobiology*, 8(2), pp.151–172. Available at: http://pubget.com/site/paper/856948?institution=fhcrc.org.

Fetcho, J.R., 1991. Spinal network of the Mauthner cell. *Brain, Behavior and Evolution*, 37(5), pp.298–316. Available at: http://pubget.com/site/paper/1933252?institution=fhcrc.org.

Goodenough, D.A. & Paul, D.L., 2009. Gap junctions. *Cold Spring Harbor perspectives in biology*, 1(1).

Güldenagel, M. et al., 2001. Visual transmission deficits in mice with targeted disruption of the gap junction gene connexin36. *The Journal of neuroscience : the official journal of the Society for Neuroscience*, 21(16), pp.6036–44. Available at: http://www.ncbi.nlm.nih.gov/pubmed/11487627.

Haas, J.S., Zavala, B. & Landisman, C.E., 2011. Activity-dependent long-term depression of electrical synapses. *Science*, 334(6054), pp.389–393. Available at:

http://www.ncbi.nlm.nih.gov/pubmed/22021860.

Hormuzdi, S.G. et al., 2004. Electrical synapses: a dynamic signaling system that shapes the activity of neuronal networks. *Biochimica et Biophysica Acta (BBA) - Biomembranes*, 1662(1–2), pp.113–137. Available at: http://linkinghub.elsevier.com/retrieve/pii/S0005273604000410.

Jacobson, G.M. et al., 2010. Connexin36 knockout mice display increased sensitivity to pentylenetetrazol-induced seizure-like behaviors. *Brain Research*, 1360, pp.198–204.

Kandarian, B. et al., 2012. The medicinal leech genome encodes 21 innexin genes: Different combinations are expressed by identified central neurons. *Development Genes and Evolution*, 222(1), pp.29–44.

Kemp, H.A., Carmany-Rampey, A. & Moens, C., 2009. Generating Chimeric Zebrafish Embryos by Transplantation. *Journal of Visualized Experiments*, (29). Available at: http://www.jove.com/index/Details.stp?ID=1394.

Kent, W.J. et al., 2002. The Human Genome Browser at UCSC. *Genome Research*, 12(6), pp.996–1006. Available at: http://www.ncbi.nlm.nih.gov/pubmed/186604%5Cnhttp://www.genome.org/cgi/doi/10.1101/gr.229102.

Kettleborough, R.N.W.R.N. et al., 2011. High-throughput target-selected gene inactivation in zebrafish. *Methods in cell biology*, 104, pp.121–127. Available at: http://pubget.com/paper/21924159?institution=fhcrc.org.

Kimmel, C.B. et al., 1995. Stages of embryonic development of the zebrafish. *Developmental dynamics : an official publication of the American Association of Anatomists*, 203(3), pp.253–310. Available at: http://eutils.ncbi.nlm.nih.gov/entrez/eutils/elink.fcgi?dbfrom=pubmed&id=8589427&retmode=ref&cmd=prlinks.

Kimmel, C.B., Sessions, S.K. & Kimmel, R.J., 1981. Morphogenesis and synaptogenesis of the zebrafish Mauthner neuron. *The Journal of comparative neurology*, 198(1), pp.101–120. Available at: http://pubget.com/site/paper/7229136?institution=fhcrc.org.

Li, H., Chuang, A.Z. & O'Brien, J., 2009. Photoreceptor coupling is controlled by connexin 35 phosphorylation in zebrafish retina. *The Journal of neuroscience : the official journal of the*

Society for Neuroscience, 29(48), pp.15178–15186. Available at: http://eutils.ncbi.nlm.nih.gov/entrez/eutils/elink.fcgi?dbfrom=pubmed&id=19955370&retmode=ref&cmd=prlinks.

Marsden, K.C. & Granato, M., 2015. In Vivo Ca2+ Imaging Reveals that Decreased Dendritic Excitability Drives Startle Habituation. *Cell Reports*, 13(9), pp.1733–1740.

Meier, C. & Dermietzel, R., 2006. Electrical synapses--gap junctions in the brain. *Results and problems in cell differentiation*, 43, pp.99–128. Available at: http://www.ncbi.nlm.nih.gov/pubmed/17068969.

Miller, A.C. et al., 2015. Neurobeachin is required postsynaptically for electrical and chemical synapse formation. *Current biology : CB*, 25(1), pp.16–28. Available at: http://www.sciencedirect.com/science/article/pii/S0960982214014195 [Accessed March 31, 2016].

Miller, A.C. et al., 2013. RNA-seq-based mapping and candidate identification of mutations from forward genetic screens. *Genome research*, 23(4), pp.679–686. Available at: http://genome.cshlp.org/cgi/doi/10.1101/gr.147322.112 [Accessed March 31, 2016].

O'Brien, J., Nguyen, H.B. & Mills, S.L., 2004. Cone photoreceptors in bass retina use two connexins to mediate electrical coupling. *The Structure of Large-Scale Synchronized Firing in Primate Retina*, 24(24), pp.5632–5642. Available at: papers3://publication/doi/10.1523/JNEUROSCI.1248-04.2004.

O'Malley, D.M., Kao, Y.H. & Fetcho, J.R., 1996. Imaging the functional organization of zebrafish hindbrain segments during escape behaviors. *Neuron*, 17(6), pp.1145–1155. Available at: http://pubget.com/site/paper/8982162?institution=fhcrc.org.

Palacios-Prado, N., Chapuis, S., et al., 2014. Molecular determinants of magnesium-dependent synaptic plasticity at electrical synapses formed by connexin36. *Nature communications*, 5, p.4667. Available at: http://www.pubmedcentral.nih.gov/articlerender.fcgi?artid=4142521&tool=pmcentrez&rendertype=abstract.

Palacios-Prado, N., Huetteroth, W. & Pereda, A.E., 2014. Hemichannel composition and electrical synaptic transmission: molecular diversity and its implications for electrical rectification. *Frontiers in cellular neuroscience*, 8(October), p.324. Available at:

http://journal.frontiersin.org/article/10.3389/fncel.2014.00324/abstract.

Pereda, A. et al., 2003. Connexin35 mediates electrical transmission at mixed synapses on Mauthner cells. *The Journal of neuroscience : the official journal of the Society for Neuroscience*, 23(20), pp.7489–7503. Available at: http://eutils.ncbi.nlm.nih.gov/entrez/eutils/elink.fcgi?dbfrom=pubmed&id=12930787&retmode=ref&cmd=prlinks.

Pereda, A.E. et al., 2004. Dynamics of electrical transmission at club endings on the Mauthner cells. *Brain research. Brain research reviews*, 47(1–3), pp.227–244. Available at: http://eutils.ncbi.nlm.nih.gov/entrez/eutils/elink.fcgi?dbfrom=pubmed&id=15572174&retmode=ref&cmd=prlinks.

Pereda, A.E., 2014. Electrical synapses and their functional interactions with chemical synapses. *Nature reviews. Neuroscience*, 15(4), pp.250–263. Available at: http://dx.doi.org/10.1038/nrn3708.

Phelan, P., 2005. Innexins: Members of an evolutionarily conserved family of gap-junction proteins. *Biochimica et Biophysica Acta - Biomembranes*, 1711(2 SPEC. ISS.), pp.225–245.

Phelan, P. et al., 2008. Molecular Mechanism of Rectification at Identified Electrical Synapses in the Drosophila Giant Fiber System. *Current Biology*, 18(24), pp.1955–1960.

Postlethwait, J. et al., 2004. Subfunction partitioning, the teleost radiation and the annotation of the human genome. *Trends in Genetics*, 20(10), pp.481–490.

Rash, J.E. et al., 2013. Molecular and Functional Asymmetry at a Vertebrate Electrical Synapse. *Neuron*, 79(5), pp.957–969.

Rash, J.E. et al., 2013. Molecular and Functional Asymmetry at a Vertebrate Electrical Synapse. *Neuron*, 79(5), pp.957–969. Available at: http://dx.doi.org/10.1016/j.neuron.2013.06.037.

Raviola, E. & Gilula, N.B., 1973. Gap Junctions Between Photoreceptor Cells in the Vertebrate Retina. *Proceedings of the National Academy of Sciences*, 70(6), pp.1677–1681. Available at: http://www.pnas.org/content/70/6/1677%5Cnhttp://www.pnas.org/content/70/6/1677.full.pdf.

Sanjana, N.E. et al., 2012. A transcription activator-like effector toolbox for genome engineering. *Nat Protoc*, 7(1), pp.171–192.

Sanjana, N.E. et al., 2012. A transcription activator-like effector toolbox for genome engineering.

Nature Protocols, 7(1), pp.171–192. Available at: http://pubget.com/site/paper/22222791?institution=fhcrc.org.

Satou, C. et al., 2009. Functional role of a specialized class of spinal commissural inhibitory neurons during fast escapes in zebrafish. *The Journal of neuroscience : the official journal of the Society for Neuroscience*, 29(21), pp.6780–6793. Available at: http://eutils.ncbi.nlm.nih.gov/entrez/eutils/elink.fcgi?dbfrom=pubmed&id=19474306&retmode=ref&cmd=prlinks.

Schindelin, J. et al., 2012. Fiji: an open-source platform for biological-image analysis. *Nature methods*, 9(7), pp.676–682. Available at: http://eutils.ncbi.nlm.nih.gov/entrez/eutils/elink.fcgi?dbfrom=pubmed&id=22743772&retmode=ref&cmd=prlinks.

Shah, A.N. et al., 2015. Rapid reverse genetic screening using CRISPR in zebrafish. *Nature methods*, 12(6), pp.535–40. Available at: http://dx.doi.org/10.1038/nmeth.3360 [Accessed March 31, 2016].

Shruti, S. et al., 2014. Electrical coupling and innexin expression in the stomatogastric ganglion of the crab *Cancer borealis*. *Journal of neurophysiology*, 112(11), pp.2946–58. Available at: http://www.ncbi.nlm.nih.gov/pubmed/25210156.

Söhl, G., Maxeiner, S. & Willecke, K., 2005. Expression and functions of neuronal gap junctions. *Nature reviews. Neuroscience*, 6(3), pp.191–200. Available at: http://www.ncbi.nlm.nih.gov/pubmed/15738956.

Söhl, G. & Willecke, K., 2004. Gap junctions and the connexin protein family. *Cardiovascular Research*, 62(2), pp.228–232.

Starich, T. a et al., 2009. Interactions between innexins UNC-7 and UNC-9 mediate electrical synapse specificity in the Caenorhabditis elegans locomotory nervous system. *Neural development*, 4, p.16.

Walker, C., Walsh, G.S. & Moens, C., 2009. Making Gynogenetic Diploid Zebrafish by Early Pressure. *Journal of Visualized Experiments*, (28). Available at: http://www.jove.com/index/Details.stp?ID=1396.

Wolman, M.A. et al., 2015. A Genome-wide Screen Identifies PAPP-AA-Mediated IGFR Signaling as a Novel Regulator of Habituation Learning. *Neuron*, 85(6), pp.1200–1211.

Wolman, M.A. et al., 2011. Chemical modulation of memory formation in larval zebrafish. *Proceedings of the National Academy of Sciences*, 108(37), pp.15468–15473. Available at: http://www.pnas.org/content/108/37/15468.short.

Yao, C. et al., 2014. Electrical synaptic transmission in developing zebrafish. *Journal of neurophysiology*, 552827(9), pp.2102–13. Available at: http://www.ncbi.nlm.nih.gov/pubmed/25080573.

Yates, A. et al., 2016. Ensembl 2016. *Nucleic Acids Research*, 44(D1), pp.D710–D716.

De Zeeuw, C.I. et al., 2003. Deformation of network connectivity in the inferior olive of connexin 36-deficient mice is compensated by morphological and electrophysiological changes at the single neuron level. *The Journal of neuroscience : the official journal of the Society for Neuroscience*, 23(11), pp.4700–11. Available at: http://www.ncbi.nlm.nih.gov/pubmed/12805309.

Zlomuzica, A. et al., 2012. Behavioral alterations and changes in Ca/calmodulin kinase II levels in the striatum of connexin36 deficient mice. *Behavioural Brain Research*, 226(1), pp.293–300.

Zoidl, G. et al., 2008. Molecular Diversity of Connexin and Pannexin Genes in the Retina of the Zebrafish Danio rerio. *Cell communication & adhesion*, 15(1–2), pp.169–183. Available at: http://informahealthcare.com/doi/abs/10.1080/15419060802014081.

Zolnik, T.A. & Connors, B.W., 2016. Electrical synapses and the development of inhibitory circuits in the thalamus. *The Journal of Physiology*, 10, p.n/a-n/a. Available at: http://doi.wiley.com/10.1113/JP271880.

Figure Legends

Fig. 1. *gjd1a/cx34.1* is required for electrical synapse formation. A. Schematic of an electrical synapse, a specialized neuronal gap junction. **B.** Simplified schematic of the zebrafish Mauthner (M) circuit in dorsal view with anterior to the left. Neurons and synapses of the hindbrain and two, of 30, spinal segments are shown. In the hindbrain mixed electrical/chemical synapses are made between auditory (Aud) afferent neurons and the M cell lateral dendrite (Aud/M electrical synapses). In the spinal cord the M axon makes electrical synapses with commissural local (CoLo) interneurons found in each segment (M/CoLo electrical synapses). **C,D.** Two representative dorsal views of spinal cord segments from *M/CoLo:GFP* larvae at 5 days post fertilization. Images are maximum intensity projections of ~10uM with anterior to the left. Scale bar = 10 uM. Larvae are stained for anti-GFP (magenta), anti-human-Connexin36 (Cx36, yellow), and for neurofilaments (RMO44, blue). Individual GFP and Cx36 channels are shown in neighboring panels. Associated experimental statistics are found in the figure-related table. The Cx36 staining found at wildtype M/CoLo synapses (**C**, red circles) is lost in *dis3* mutants (**D**, red circles). **E.** Genome wide RNA-seq-based mapping data. The average frequency of mutant markers (black marks) is plotted against genomic position. A single region on chromosome 5 (chr5) emerges with an allele frequency near 1.0 indicating linkage to the *dis3* mutation (red arrow). Each chromosome is separated by vertical lines and labeled at the bottom. **F.** Mutant reads from the RNA-seq mapping data at two separate positions within the *gjd1a/cx34.1* gene are shown aligned to the reference genome identifying two missense changes within *dis3* mutant animals. Wildtype reference (ref) genome nucleotides and encoded amino acids (aa) are noted. Aligned mutant (MUT) reads are shown as grey boxes; colored letters highlights differences from reference. **G.** Electrical synapses are lost in trans-heterozygous animals carrying a *dis3* and an 8-bp frameshift allele (*dis3/8bp)* in *gjd1a/cx34.1*. Images of the spinal cord as in C,D.

Fig. 2. The zebrafish genome encodes four Connexin-encoding genes related to mammalian *gjd2/cx36*. A. Amino acid alignment of four zebrafish Cx36-like proteins with human Cx36. Colored lines indicate approximate location of the domains shown in the schematic in B. **B.** Schematic of Cx36-like proteins. Blue: extracellular (EC) loops; grey cylinders: transmembrane (TM) domains; black: intracellular N- and C-terminal tails; magenta: intracellular (IL) loop. Red stars indicate the positions of mutations in ENU-induced (*fh329, fh360*) and engineered (*fh435, fh436, fh437, fh454*) mutations in the four zebrafish genes encoding Cx36-like proteins: *gjd1a/cx34.1, 1b/cx34.7, 2a/cx35.5,* and *2b/cx35.1.* Details of mutations can be found in the figure-related table. **C.** Phylogeny of vertebrate Cx36 proteins. *Gjd2a* and *2b* are duplicates of the single mammalian gene encoding Cx36. *Gjd1a* and *1b* are duplicates of a gene that was lost in the tetrapod lineage. Lamprey = *Petromyzon marinus*, duck = Anas platyrhynchos, lizard = Anolis carolinensis, toad = Xenopus tropicalis, mouse = Mus musculus, rat = Rattus norvegicus, human = *Homo sapiens*, zfish = *Danio rerio*.

Fig. 3. Electrical synapses of the Mauthner circuit require both *gjd1a/cx34.1* and *gjd2a/cx35.5*. A-I. In this and all subsequent figures, unless otherwise specified, images are dorsal views of hindbrain, Mauthner lateral dendrite, and two spinal cord segments from *M/CoLo:GFP* larvae at 5 days post fertilization. Hindbrain, lateral dendrite, and spinal cord images are maximum intensity projections of ~30, ~5, and ~10uM, respectively. Anterior is to the left. Scale bar = 10 uM. Larvae are stained for anti-GFP (magenta), anti-human-Connexin36 (Cx36, yellow), and for neurofilaments (RMO44, blue). Individual GFP and Cx36 channels are shown in neighboring

panels. Electrical synapses are found on the Mauthner cell body (**A**) with prominent and stereotyped Aud/M synapses found on Mauthner's lateral dendrite (arrows in **A**, **B**) and at M/CoLo synapses in the spinal cord (**C**, red circles). (**D-I**) In *gjd1a/cx34.1* and *gjd2a/cx35.5* mutants Mauthner electrical synapses are lost or, in the specific case of Aud/M synapses in *gjd1a/cx34.1* mutants, diminished. **J-L.** Bar graphs represent the mean of the indicated value quantified at synapses with each circle representing the average of 12-16 M/CoLo or 8-12 Aud/M synapses within an animal. **J,K.** M/CoLo electrical synapses are absent in *gjd1a/cx34.1* and *gjd2a/cx35.5* mutants, while Aud/M club endings are strongly reduced in *gjd1a* mutants and absent in *gjd2a* mutants. *gjd1b* and *gjd2b* have no effect on Mauthner electrical synapses. N = **L.** The remaining Cx36 staining observed at Aud/M synapses in *gjd1a* mutants is not due to *gjd1b* or *gjd2b*. For reference, the first bar is a duplication of *gjd1a* mutant data from K. In *gjd1a;gjd2a* double mutants the remaining Cx36 staining is lost as expected given that *gjd2a* is required for Aud/M synapses (K). In double and triple mutants combinations between *gjd1a*, *gjd1b,* and *gjd2b* there is no effect on the remaining Cx36 staining at Aud/M synapses. Associated experimental statistics are found in the figure-related table.

Fig. 4. Electrical synapses are functionally defective in *gjd1a/cx34.1* and *gjd2a/cx35.5* mutants. Retrograde labeling of Mauthner axons with the gap junction permeable dye Neurobiotin (Nb) from a caudal transection. Hindbrain and spinal cord images are maximum intensity projections of ~30 and ~10uM, respectively. Anterior is to the left. Scale bar = 10 uM. Spinal cord images are at the level of the CoLo cell bodies (circles), which is dorsal to the synapses. **A-F.** Larvae are stained for anti-GFP (magenta), biotin (Nb, cyan), and anti-human-Connexin36 (Cx36, yellow). Nb labels the Mauthner cell bodies and other caudally projecting neurons in the hindbrain (**A**) and passes from the Mauthner axon through the electrical synapses to fill the CoLo cell bodies (**B**, circles). Other neurons are also labeled due to projections caudally into the lesion site (A, non-Mauthner neurons, B, non-circled cell bodies). **C-F.** In *gjd1a/cx34.1* and *gjd2a/cx35.5* mutants Nb labels M normally (C,E) however none passes into CoLos (D,F). **G.** Quantitation of the ratio of Nb in CoLo to M cell bodies in wildtype and mutants. Each circle represents the average Nb fluorescence within 8-12 CoLo cell bodies compared to the 2 Mauthner cell bodies in an animal. Associated experimental statistics are found in the figure-related table.

Fig. 5: Recruitment of Gjd1a/Cx34.1 and Gjd2a/Cx35.5 to electrical synapses is co-dependent. Larvae are stained for anti-GFP (magenta), anti-Connexin34.1 (Cx34.1, yellow), and for anti-Connexin35.5 (Cx35.5, cyan). Individual Cx34.1 and Cx35.5 channels are shown in neighboring panels. Hindbrain, lateral dendrite, and spinal cord images are maximum intensity projections of ~30, ~5, and ~10uM, respectively. Anterior is to the left. Scale bar = 10 uM. **A-C.** Cx34.1 and Cx35.5 are found colocalized at electrical synapses throughout the hindbrain (A) including at Aud/M (arrows in A, B), and M/CoLo synapses (C). In *gjd1a/cx34.1* mutants the localization of Cx35.5 to electrical synapses is lost (**D-F**) or diminished at Aud/M synapses (E); in *gjd2a/cx35.5* mutants the localization of Cx34.1 to electrical synapses is lost (**G-I**). Associated antibody information is found in the figure-related table.

Fig. 6: *gjd1a/cx34.1* and *gjd2a/cx35.5* are required asymmetrically at Mauthner electrical synapses. Dorsal views of chimeric larvae containing Biotin-Dextran- (BD) or GFP-marked cells transplanted from a donor embryo of noted genotype into a wildtype (wt) host; throughout the figure the neurons derived from the donor embryo are displayed in magenta, while those from the host

are in blue. Synapses (stained with anti-human-Cx36, yellow) associated with a transplanted neuron (cyan circles and boxes) can be directly compared to wildtype host synapses (red circles and boxes). Hindbrain, lateral dendrite, and spinal cord images are maximum intensity projections of ~30, ~5, and ~10uM, respectively. Anterior is to the left. Scale bar = 10 uM. **A-C**. At the Aud/M synapses presynaptic auditory afferent neurons (in A, stained with BD, magenta) synapse onto the postsynaptic Mauthner lateral dendrite (stained with anti-GFP, blue in A, magenta in B,C). **D,E.** At the M/CoLo synapses the presynaptic Mauthner axon (stained with anti-GFP, magenta in D) synapses with the postsynaptic CoLo (stained with anti-GFP, magenta in E). **F-J.** Presynaptic removal of *gjd1a/cx34.1* function has no effect on Aud/M and M/CoLo synapses (cyan circles in **F,I**). By contrast, removing *gjd1a/cx34.1* postsynaptically causes a loss of electrical synapse staining (cyan boxes and circles in **G,H,J**; note residual Cx36 staining at Aud/M synapses when *gjd1a/cx34.1* is removed from only the postsynaptic neuron, H). **K-O.** Conversely, *gjd2a/cx35.5* function is required exclusively presynaptically (**K,N**) and is dispensable postsynaptically (**L,M,O**). **P,Q.** Quantitation of the ratio of Cx36 at donor-associated synapses to wildtype host synapses in chimaeric embryos. Each circle represents the average ratio of 1-8 donor-associated to 8-12 host-associated synapses within an animal, varying depending on the synapse and chimaera. Associated experimental statistics are found in the figure-related table.

Fig. 7: The exclusive asymmetric functions of *gjd1a/cx34.1* and *gjd2a/cx35.5* are sufficient for electrical synapse formation. Dorsal views of chimeric larvae containing GFP-marked cells transplanted from a wildtype (wt) donor embryo into a mutant host of noted genotype; throughout the figure the neurons derived from the wt donor embryo are displayed in magenta, while those from the mutant host are in blue. Synapses (stained with anti-human-Cx36, yellow) associated with a transplanted neuron (cyan circles and boxes) can be directly compared to mutant host synapses (red circles and boxes). Hindbrain, lateral dendrite, and spinal cord images are maximum intensity projections of ~30, ~5, and ~10uM, respectively. Anterior is to the left. Scale bar = 10 uM. **A-D**. When the postsynaptic neuron of the Aud/M or M/CoLo synapse is wildtype in a *gjd1a/cx34.1* mutant the electrical synapses are rescued (A,B,D). By contrast, when the presynaptic neuron is wildtype in a mutant there is no effect on Cx36 staining at the synapse (C). **E-H.** Conversely, electrical synapses are rescued in *gjd2a/cx35.5* mutants only when the presynaptic, and not the postsynaptic, neuron is wildtype. **I,J.** Quantitation of the fold increase in the ratio of Cx36 at wt-donor-associated synapses to mutant host synapses in chimaeric embryos. Each circle represents the average ratio of 1-8 donor-associated to 8-16 host-associated synapses within an animal. Associated experimental statistics are found in the figure-related table.

Fig. 8: *gjd1a/cx34.1* and *gjd2a/cx35.5* mutants have delayed and abnormal escape responses. M-induced escape responses (Short Latency C-bends, SLCs) to a startling vibrational (sound) stimuli executed by 6 day post fertilization larvae were analyzed by high-speed (1000 frame per second) videomicroscopy. Scale bar = 1 mM. **A.** Frequency of elicited SLCs in wildtype (wt) and indicated mutants in 10 trials per animal. Note that the FLOTE analysis software removes some trials if they cannot be classified. Bar graphs represent data as mean +/- SEM with each circle representing an individual animal's average % of response. Mutant larvae execute escapes as frequently as WT (n = 52, 20, & 29 larvae for wt, *gjd1a/cx34.1*, & *gjd2a/cx35.5*, respectively; 1 way ANOVA not significant (ns), Dunn's Multiple Comparison Test: wt to *gjd1a/cx34.*1 & wt to *gjd2a/cx35.5* both ns). **B.** Latency of elicited SLCs in all individual trials. Bar graphs represent data as mean +/- SEM with each circle representing individual SLC latencies. Mutant larvae are

significantly delayed in their latency to initiate an M-induced SLC (n= 359, 160, & 180 SLCs from 52, 20, & 29 larvae from wt, *gjd1a/cx34.1*, & *gjd2a/cx35.5*, respectively; 1 way ANOVA $P < 0.0001$, Dunn's Multiple Comparison Test: wt to *gjd1a/cx34.*1 & wt to *gjd2a/cx35.5* both significant at $P < 0.001$). **C,D**. Kinematic analysis of the maximum SLC turn angle (C) and angular velocity (D) plotted as the average number of events within an indicated bin. Arrows indicate shallow angle and low velocity turns exhibited by mutants. **E-H**. Time-lapse analysis of a normal (E,F) and delayed (G,H) M-induced escape response (SLCs). Individual snapshots taken at the indicated times (ms = milliseconds) are overlaid on an individual image (E,G). A line representing the midline body axis at each time was drawn by hand to indicate the movement (F,H). **I-L.** A normal escape bend at its maximum angle (I) compared to abnormally shaped escape bends executed by *gjd1a* (J,K) or *gjd2a* (L) mutant larvae. Associated experimental statistics are found in the figure-related table.

Fig. 9: Schematics of the asymmetric functions of Cx proteins at zebrafish electrical synapses. A. Model of an electrical synapse with an exclusive pre- and postsynaptic Cx making up the gap junction plaque. We provide genetic evidence of this asymmetry at Mauthner synapses but it is likely broadly used in the nervous system. Such asymmetry is likely to drive functional asymmetry at these synapses (see discussion). **B.** Model of asymmetric electrical synapses found in concert with chemical synapses of the Mauthner circuit. The electrical synapses contribute speed and coordination to circuit function. The speed is likely imparted via the Aud/M synapses in the hindbrain while the coordination is likely via the M/CoLo synapses in the spinal cord (see discussion).

Fig.1

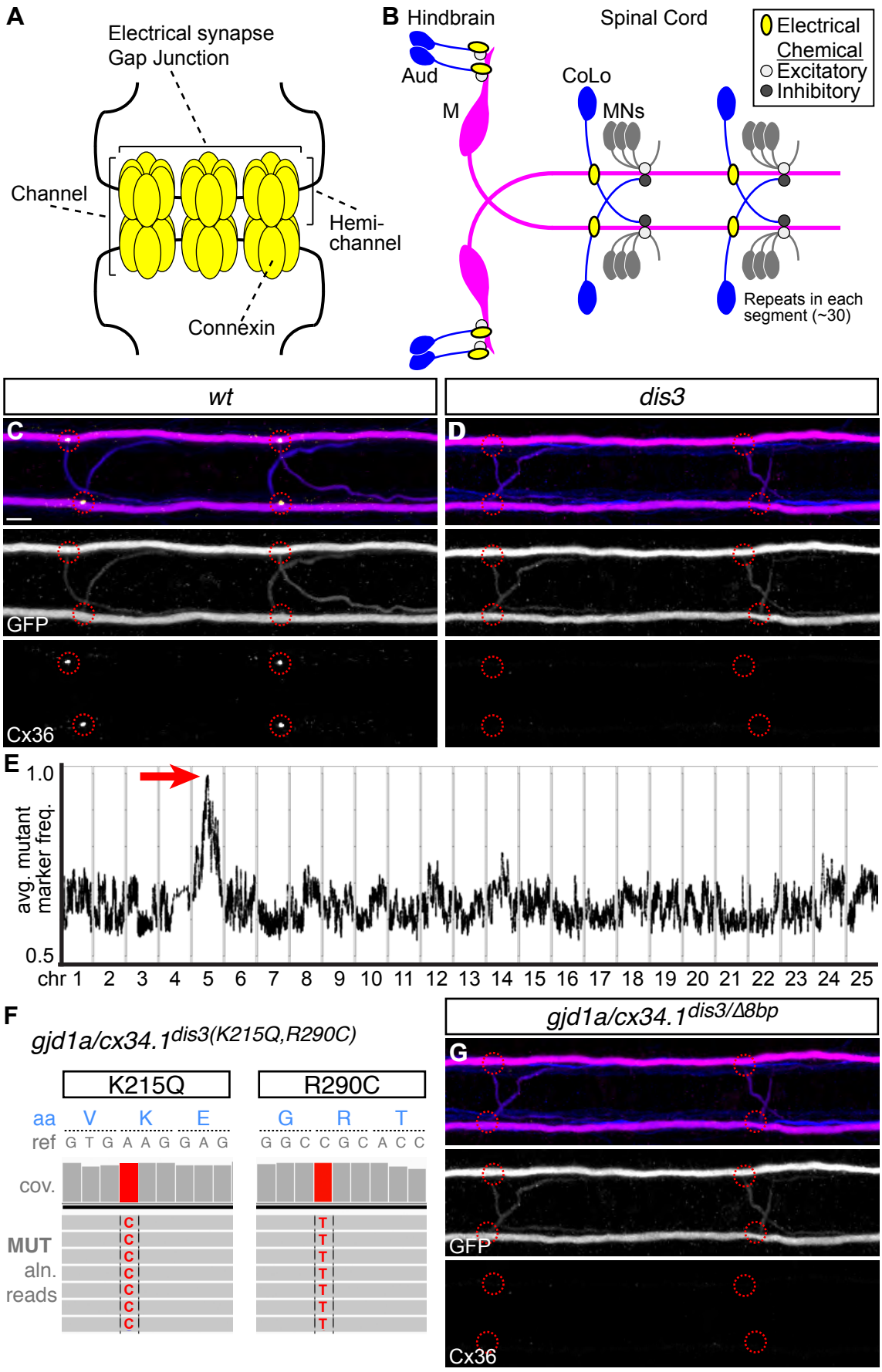

Fig.2

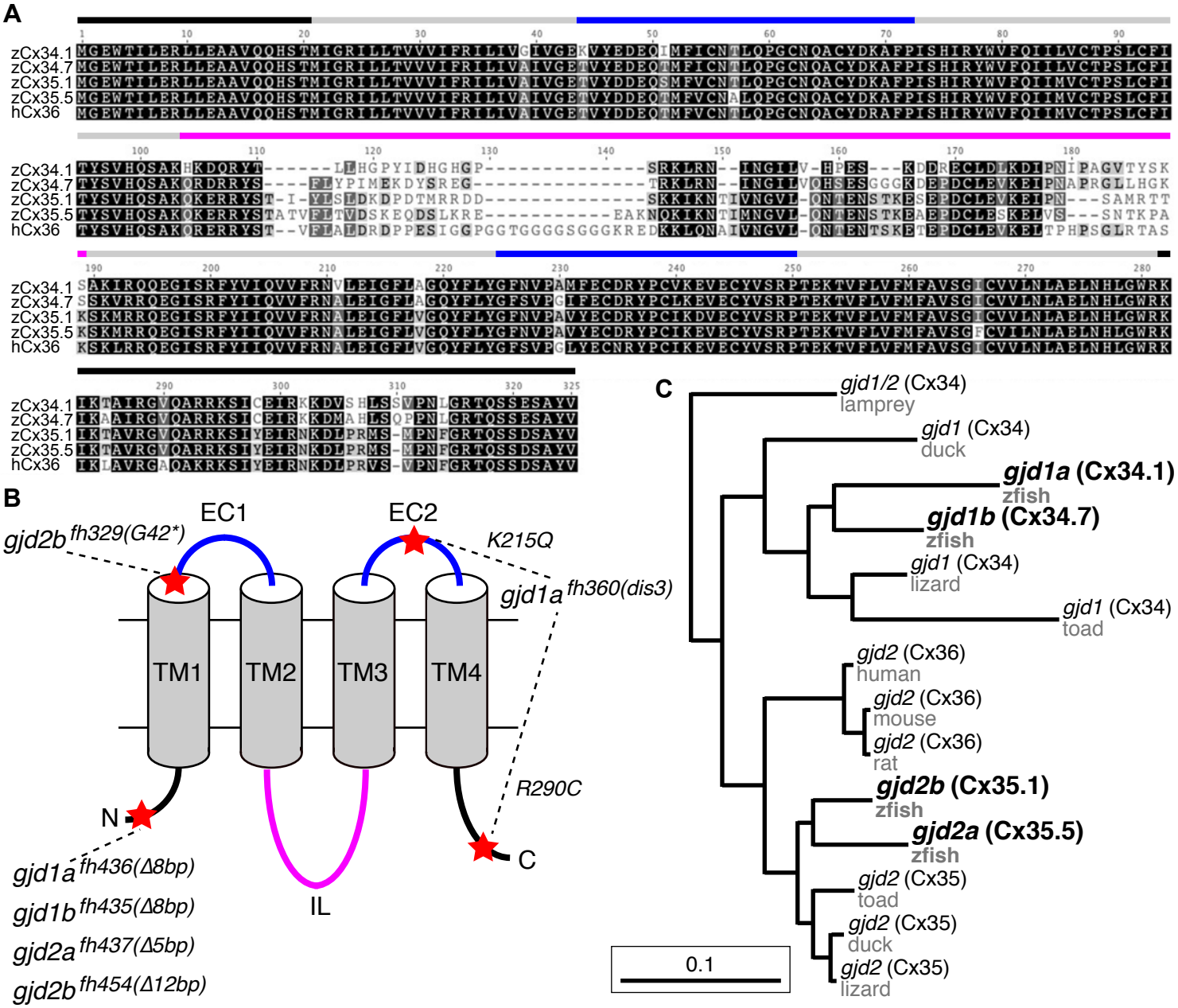

Fig.3

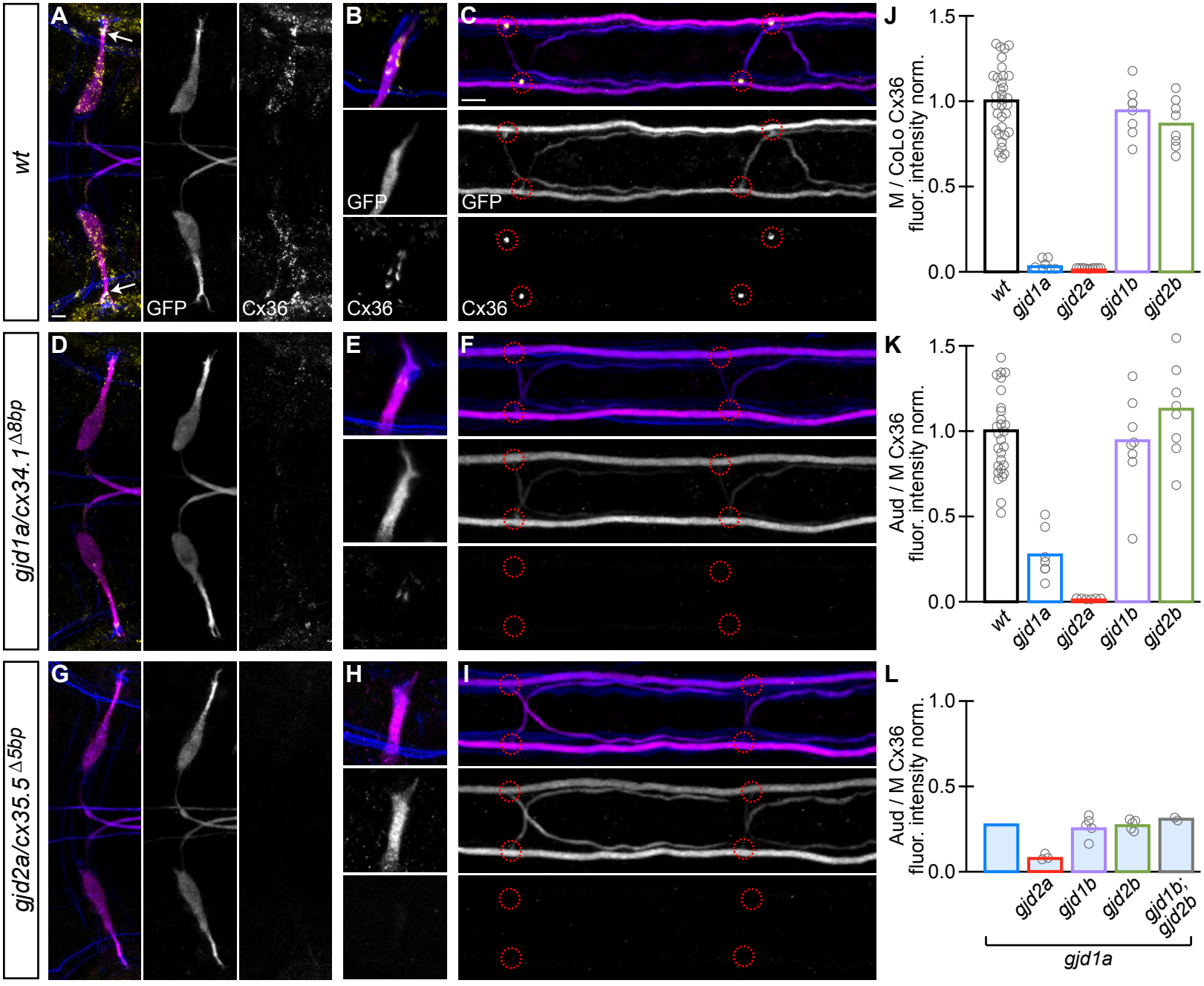

Fig.4

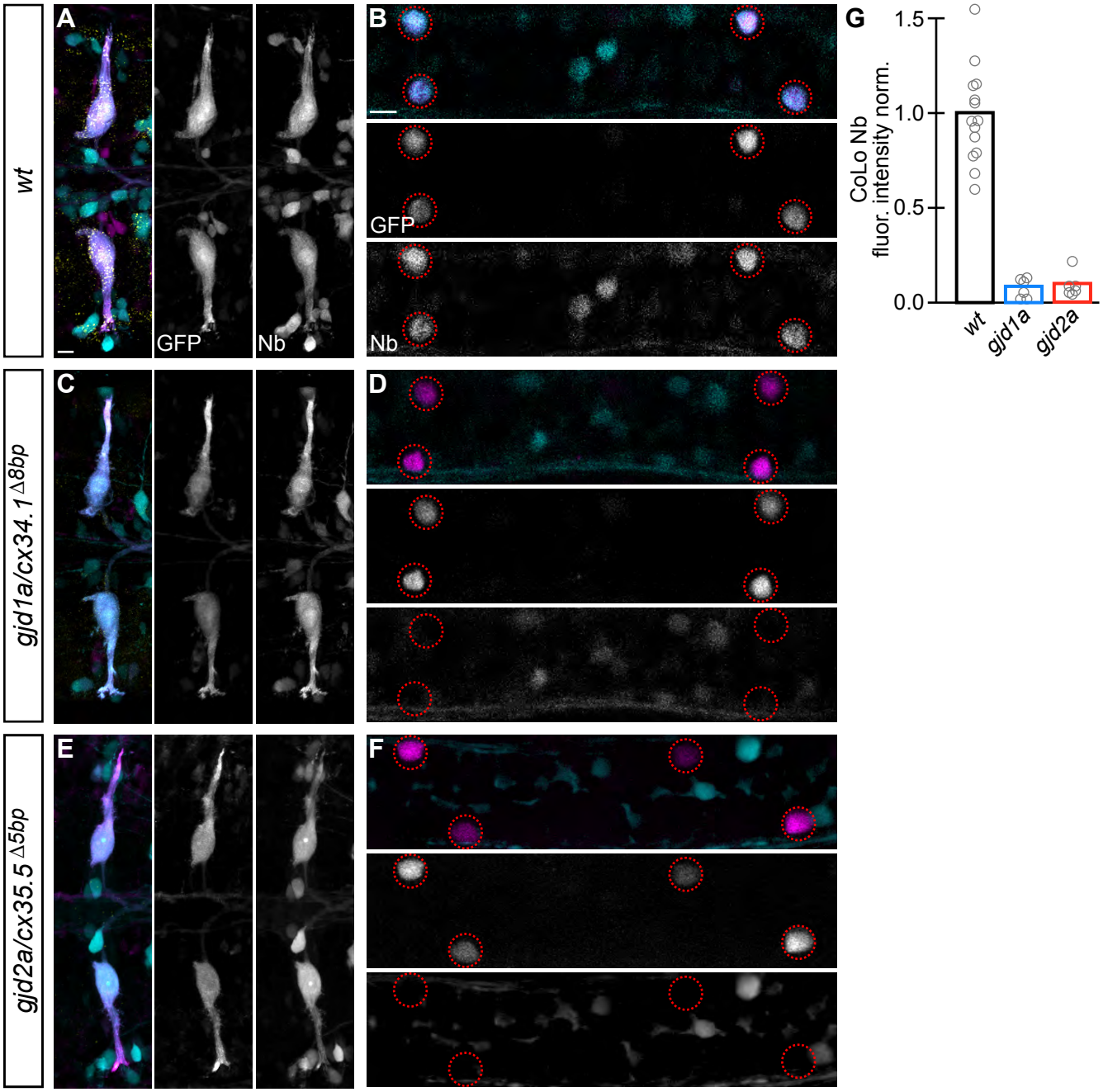

Fig.5

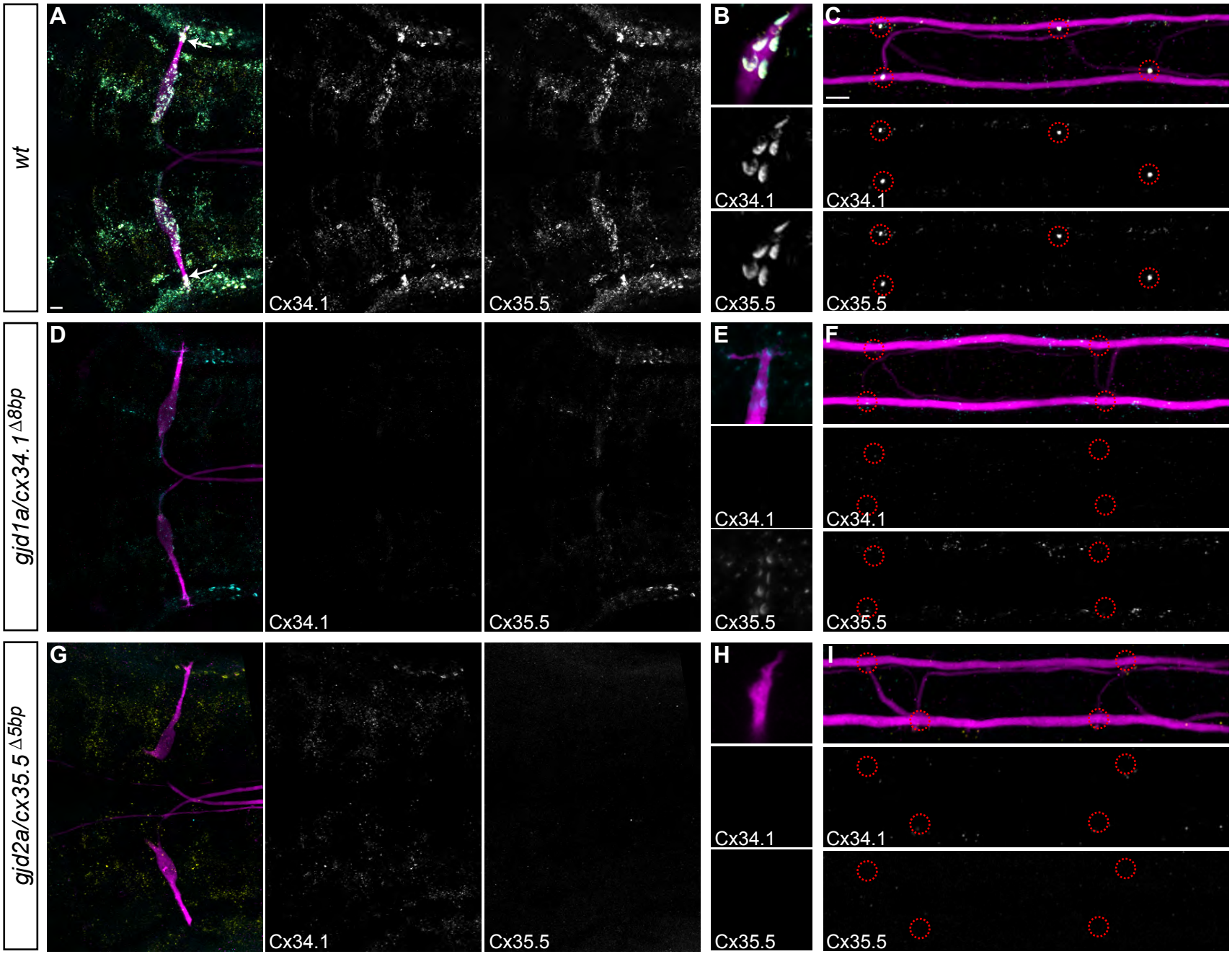

Fig.6

Aud/M

M/CoLo

Presynaptic Aud

Postsynaptic M

Presynaptic M

Postsynaptic CoLo

wt > *wt* host

gjd1a/cx34.1 > *wt* host

gjd2a/cx35.5 > *wt* host

A

B

C

D

E

F

G

H

I

J

K

L

M

N

O

Cx36

GFP

BD

P

Aud / M Cx36 fluor. intensity norm.

1.5

1.0

0.5

0.0

pre

post

wt

gjd1a

gjd2a

Q

M / CoLo Cx36 fluor. intensity norm.

Fig.7

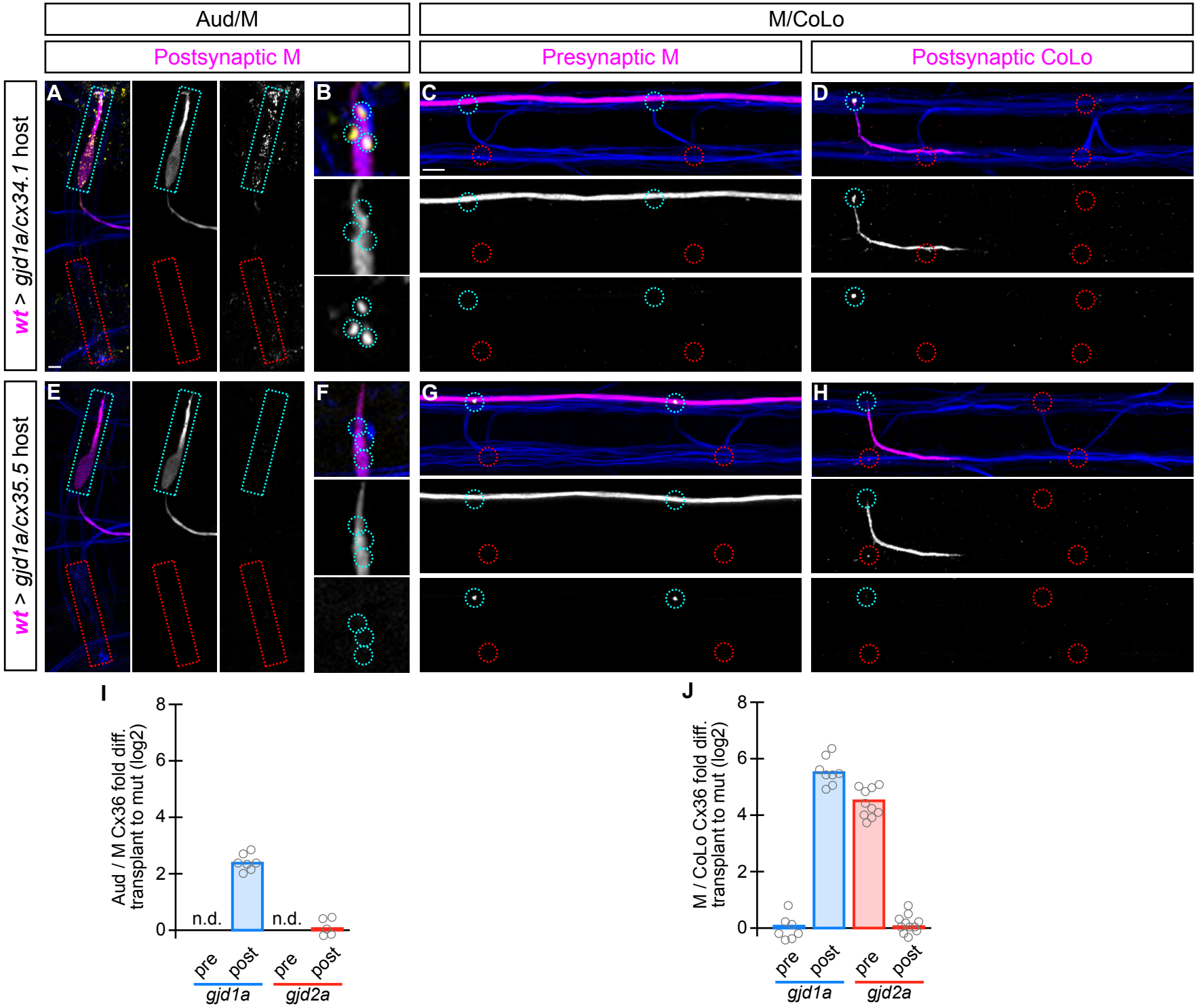
Aud/M
M/CoLo
Postsynaptic M
Presynaptic M
Postsynaptic CoLo
wt > gjd1a/cx34.1 host
wt > gjd1a/cx35.5 host
A
B
C
D
E
F
G
H
I
Aud / M Cx36 fold diff.
transplant to mut (log2)
n.d.
n.d.
pre
post
pre
post
gjd1a
gjd2a
J
M / CoLo Cx36 fold diff.
transplant to mut (log2)
pre
post
pre
post
gjd1a
gjd2a

Fig.8

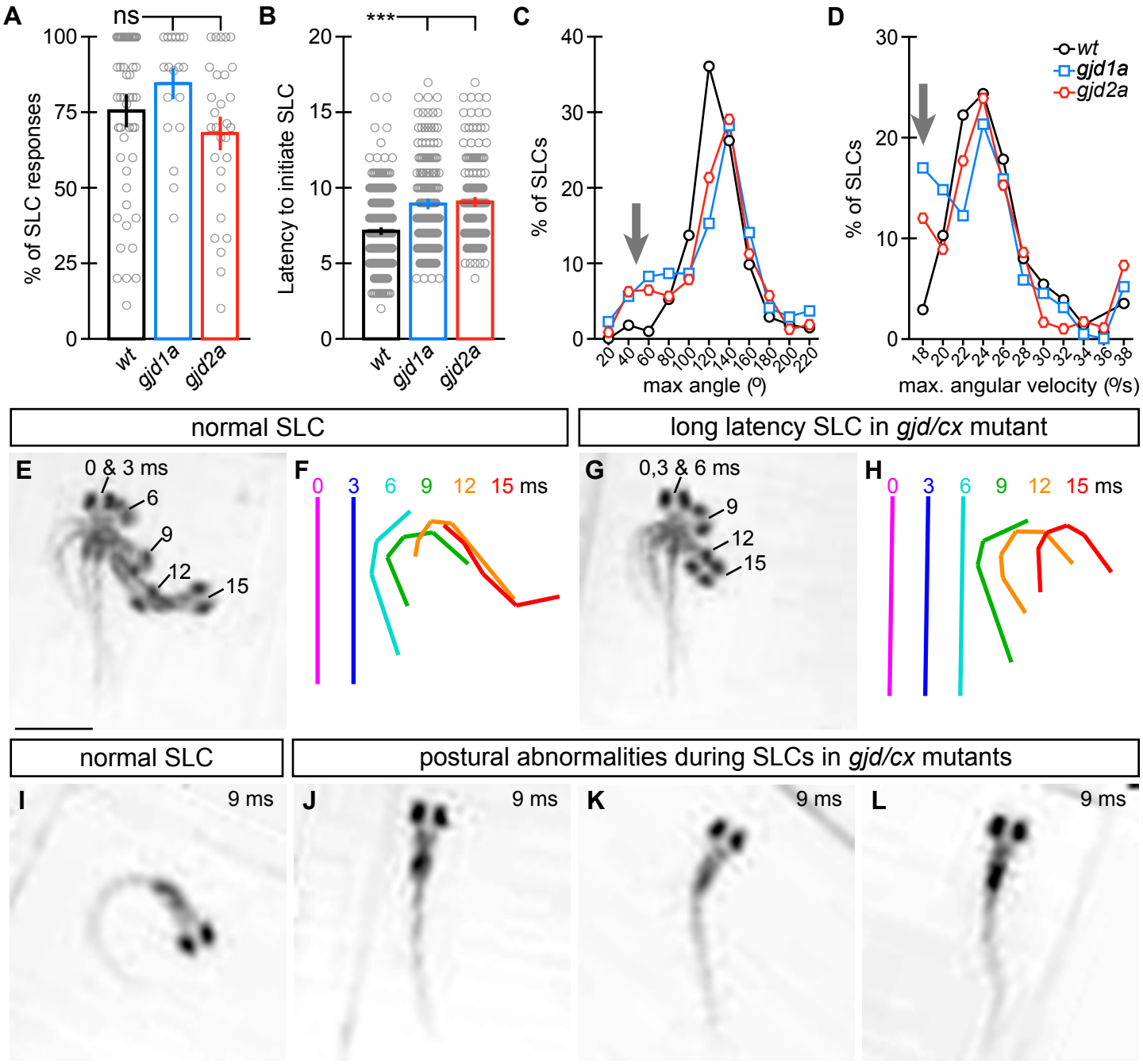

Fig.9

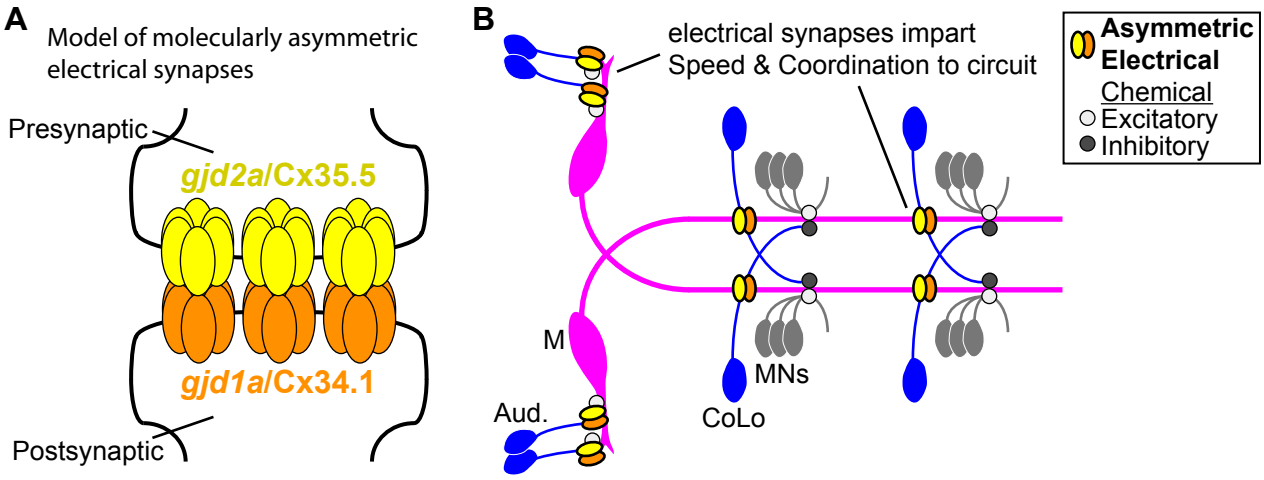

Fig. 1

M/CoLo - spinal cord

gjd1a$^{dis3/+}$ X gjd1a$^{\Delta 8bp/+}$

	anti-Cx36			
	wt	**gjd1a $^{dis3\ /\ +}$**	**gjd1a $^{\Delta 8bp\ /\ +}$**	**gjd1a $^{dis3\ /\ \Delta 8bp}$**
avg. for anima	10.45	8.62	10.95	0.05
	10.78	7.21	14.85	0.11
	12.86	7.56	12.29	0.05
	13.62	7.40	9.14	0.04
	12.28	7.19	12.74	0.08
	16.45	7.05	12.32	0.06
		6.60	12.26	0.07
avg.	12.74	7.38	12.08	0.07
stdev	2.18	0.63	1.74	0.02
sterr	0.89	0.24	0.66	0.01
n	6.00	7.00	7.00	7.00

	anti-Cx36 - NORMALIZED to wt average			
	wt	**gjd1a $^{dis3\ /\ +}$**	**gjd1a $^{\Delta 8bp\ /\ +}$**	**gjd1a $^{dis3\ /\ \Delta 8bp}$**
avg. for anima	0.82	0.68	0.86	0.00
	0.85	0.57	1.17	0.01
	1.01	0.59	0.96	0.00
	1.07	0.58	0.72	0.00
	0.96	0.56	1.00	0.01
	1.29	0.55	0.97	0.00
		0.52	0.96	0.01
avg.	1.00	0.58	0.95	0.01
stdev	0.17	0.05	0.14	0.00
sterr	0.07	0.02	0.05	0.00
n	6.00	7.00	7.00	7.00

- each avg. for animal represents 12-16 individual M/CoLo synapses

Fig. 2

chr	gene	Ensembl ID	protein	mutations	nucleotide change	wt sequence #1	mutant sequence #1	wt sequence #2	mutant sequence #2	predicted consequence	notes
5	gjd1a	ENSDARG00000035340	Cx34.1	fh360 (dis3)	K215Q, R290C	CGTGAAGGAGGTTGAATGTTACGTG	CGTGCAGGAGGTTGAATGTTACGTG	TGGGCCGCACCCAGTCTAGCGAATC	TGGGCTGCACCCAGTCTAGCGAATC	two amino acid changes	The ENU mutagensis produced two missense mutations in gjd1a. We have not resolved causation to one or both mutations.
				fh436	Δ8bp starting at nt 5	**ATG**GGAGAATGGACTATATTGGAGA	**ATG**GACTATATTGGAGAGGTTGCTG			encodes an entirely different, frame-shifted, peptide truncating after 43aas	
15	gjd1b	ENSDARG00000035765	Cx34.7	fh435 (Δ8bp)	Δ8bp starting at nt 2	**ATG**GGAGAGTGGACCATTTTAGAGC	**ATG**GACCATTTTAGAGCGCCTCCTG			encodes an entirely different, frame-shifted, peptide truncating after 34aas	
17	gjd2a	ENSDARG00000067999	Cx35.5	fh437 (Δ5bp)	Δ5bp starting at nt 20	**ATG**GGAGAATGGACCATACTAGAGA	**ATG**GGAGAATGGACCATACAGGCTC			change at L7Q followed by frame-shifted peptide truncating after 42aas	The contigs of the genome are misalgned in this region of GRCz10. On Ensembl only exon2 is annotated. Exon 1 is present but is found downstream of exon 2. However, a full length, exon1-exon2 cDNA was cloned from an RNA library.
20	gjd2b	ENSDARG00000070781	Cx35.1	fh329	G42*	TTGTTGGAGAGACCGTGTACGACGA	TTGTTTGAGAGACCGTGTACGACGA			truncated after first transmembrane domain	
				fh454	Δ12bp starting in 5'UTR and deleting A of ATG	ATTCGCCTCCGAATGAACAGCC**ATG**	TCTCTGTGTTACATTCGCCTCCGTG			nearest ATG is 7bp downstream and would encode a entirely different, frame-shifted, peptide truncating after 53aas	

- underlined sections of wt sequence denote nucleotides that are effected in mutant sequence
- start codons are in bold
- aa = amino acid

Fig.3

M/CoLo - spinal cord

gjd1a^{fh436} Δ8bp incross

gjd1a 8bp (fh436) het incross

anti-Cx36 - RAW pixel values

	wt	gjd1a $^{\Delta 8bp/+}$	gjd1a $^{\Delta 8bp/\Delta 8bp}$
avg. for animal	17.65	21.72	0.25
	10.28	3.97	0.17
	12.69	14.63	0.36
	19.29	18.26	1.02
	16.35	14.72	0.44
	15.45	17.72	0.19
	20.07	13.34	1.07
	10.59	21.33	
avg.	15.30	15.71	0.50
stdev	3.77	5.65	0.38
sterr	1.33	2.00	0.15
n	8.00	8.00	7.00

anti-Cx36 - NORMALIZED to wt avg.

	wt	gjd1a $^{\Delta 8bp/+}$	gjd1a $^{\Delta 8bp/\Delta 8bp}$
avg. for animal	1.15	1.42	0.02
	0.67	0.26	0.01
	0.83	0.96	0.02
	1.26	1.19	0.07
	1.07	0.96	0.03
	1.01	1.16	0.01
	1.31	0.87	0.07
	0.69	1.39	
avg.	1.00	1.03	0.03
stdev	0.25	0.37	0.03
sterr	0.09	0.13	0.01
n	8.00	8.00	7.00

gjd1a^{fh360} dis3 incross

gjd1a dis3 (fh360) het incross

anti-Cx36 - RAW pixel values

	wt	gjd1a $^{dis3/+}$	gjd1a $^{dis3/dis3}$
avg. for animal	12.06	5.78	2.34
	16.78	8.72	0.88
	15.99	6.43	0.47
	17.86	6.06	0.51
	10.14	9.19	0.33
	10.33	5.64	1.05
	10.43	9.27	0.91
	14.8	3.99	1.87
	15.77	7.74	2.18
	18.81	8.02	1.45
avg.	14.30	7.08	1.20
stdev	3.29	1.76	0.73
sterr	1.04	0.56	0.23
n	10.00	10.00	10.00

anti-Cx36 - NORMALIZED to wt avg.

	wt	gjd1a $^{dis3/+}$	gjd1a $^{dis3/dis3}$
avg. for animal	0.84	0.40	0.16
	1.17	0.61	0.06
	1.12	0.45	0.03
	1.25	0.42	0.04
	0.71	0.64	0.02
	0.72	0.39	0.07
	0.73	0.65	0.06
	1.04	0.28	0.13
	1.10	0.54	0.15
	1.32	0.56	0.10
avg.	1.00	0.50	0.08
stdev	0.23	0.12	0.05
sterr	0.07	0.04	0.02
n	10.00	10.00	10.00

gjd2a^{fh437} Δ5bp incross

gjd2a 5bp (fh437) het incross

anti-Cx36 - RAW pixel values

	wt	gjd2a $^{\Delta 5bp/+}$	gjd2a $^{\Delta 5bp/\Delta 5bp}$
avg. for animal	12.97	20.87	0.33
	26.83	27.95	0.17
	30.16	22.37	0.3
	25.5	20.58	0.13
	29.47	26.66	0.23
	36.32	17.35	0.14
	28.3	22	0.11
	22.33	22.63	0.4
	24.84	20.96	0.29
	36.02	28.86	0.27
avg.	27.27	23.02	0.24
stdev	6.76	3.66	0.10
sterr	2.14	1.16	0.03
n	10.00	10.00	10.00

anti-Cx36 - NORMALIZED to wt avg.

	wt	gjd2a $^{\Delta 5bp/+}$	gjd2a $^{\Delta 5bp/\Delta 5bp}$
avg. for animal	0.48	0.77	0.01
	0.98	1.02	0.01
	1.11	0.82	0.01
	0.93	0.75	0.00
	1.08	0.98	0.01
	1.33	0.64	0.01
	1.04	0.81	0.00
	0.82	0.83	0.01
	0.91	0.77	0.01
	1.32	1.06	0.01
avg.	1.00	0.84	0.01
stdev	0.25	0.13	0.00
sterr	0.08	0.04	0.00
n	10.00	10.00	10.00

gjd1b^{fh435} Δ8bp incross

gjd1b 8bp (fh435) het incross

anti-Cx36 - RAW pixel values

	wt	gjd1b $^{\Delta 8bp/+}$	gjd1b $^{\Delta 8bp/\Delta 8bp}$
avg. for animal	5.01	6.89	6.18
	5.82	7.76	5.96
	5.09	6	5.45
	6.11	5.32	4.49
	6.12	5.93	5.14
	7.52	5.11	6.54
	7.18	6.92	7.37
	6.39	5.89	6.18
	7.15		
avg.	6.27	6.23	5.91
stdev	0.90	0.89	0.89
sterr	0.30	0.32	0.31
n	9.00	8.00	8.00

anti-Cx36 - NORMALIZED to wt avg.

	wt	gjd1b $^{\Delta 8bp/+}$	gjd1b $^{\Delta 8bp/\Delta 8bp}$
avg. for animal	0.80	1.10	0.99
	0.93	1.24	0.95
	0.81	0.96	0.87
	0.98	0.85	0.72
	0.98	0.95	0.82
	1.20	0.82	1.04
	1.15	1.10	1.18
	1.02	0.94	0.99
	1.14		
avg.	1.00	0.99	0.94
stdev	0.14	0.14	0.14
sterr	0.05	0.05	0.05
n	9.00	8.00	8.00

gjd2b^{fh329} G42* incross

gjd2b G42* (fh329) het incross

anti-Cx36 - RAW pixel values

	wt	gjd2b $^{G42*/+}$	gjd2b $^{G42*/G42*}$
avg. for animal	19.63	17.59	18.42
	13.02	16.44	12.71
	12.02	16.04	16.4
	14.59	18.27	15.82
	12.4	14.99	17.32
	24.6	19.1	13.64
	17.68	15.42	11.7
	22.88	15.77	13.16
avg.	17.10	16.70	14.90
stdev	4.89	1.46	2.42
sterr	1.73	0.52	0.86
n	8.00	8.00	8.00

anti-Cx36 - NORMALIZED to wt avg.

	wt	gjd2b $^{G42*/+}$	gjd2b $^{G42*/G42*}$
avg. for animal	1.15	1.03	1.08
	0.76	0.96	0.74
	0.70	0.94	0.96
	0.85	1.07	0.93
	0.73	0.88	1.01
	1.44	1.12	0.80
	1.03	0.90	0.68
	1.34	0.92	0.77
avg.	1.00	0.98	0.87
stdev	0.29	0.09	0.14
sterr	0.10	0.03	0.05
n	8.00	8.00	8.00

gjd2b^{fh456} Δ12bp incross

gjd2b 12bp (fh454) het incross

anti-Cx36 - RAW pixel values

	wt	gjd2b $^{\Delta 12bp/+}$	gjd2b $^{\Delta 12bp/\Delta 12bp}$
avg. for animal	n.d.	n.d.	n.d.
avg.			***
stdev			
sterr			
n			

anti-Cx36 - NORMALIZED to wt avg.

	wt	gjd2b $^{\Delta 12bp/+}$	gjd2b $^{\Delta 12bp/\Delta 12bp}$
avg. for animal	n.d.	n.d.	n.d.
avg.			***
stdev			
sterr			
n			

Aud/M - club ending, hindbrain

gjd1a^{fh436} Δ8bp incross

anti-Cx36 - RAW pixel values

	wt	gjd1a $^{\Delta 8bp/+}$	gjd1a $^{\Delta 8bp/\Delta 8bp}$
avg. for animal	27.63	15.62	4.85
	13.27	16.73	5.84
	26.94	24.86	13.05
	26.60	30.37	11.27
	24.51	29.44	4.87
	28.86	22.84	2.58
	25.48	17.13	6.58
	33.98	29.79	
avg.	25.91	23.35	7.01
stdev	5.86	6.24	3.76
sterr	2.07	2.21	1.42
n	8.00	8.00	7.00

anti-Cx36 - NORMALIZED to wt avg.

	wt	gjd1a $^{\Delta 8bp/+}$	gjd1a $^{\Delta 8bp/\Delta 8bp}$
avg. for animal	1.07	0.60	0.19
	0.51	0.65	0.23
	1.04	0.96	0.50
	1.03	1.17	0.43
	0.95	1.14	0.19
	1.11	0.88	0.10
	0.98	0.66	0.25
	1.31	1.15	
avg.	1.00	0.90	0.27
stdev	0.23	0.24	0.15
sterr	0.08	0.09	0.05
n	8.00	8.00	7.00

gjd1a^{fh360} dis3 incross

anti-Cx36 - RAW pixel values

	wt	gjd1a $^{dis3/+}$	gjd1a $^{dis3/dis3}$
avg. for animal	13.32	20.66	6.41
	19.47	22.25	5.97
	26.45	23.76	6.46
	25.40	15.00	7.29
	21.54	17.91	3.03
	20.37	14.19	3.56
	20.76	11.52	2.83
	24.07	11.65	1.58
	11.89	11.24	4.07
	18.55		3.48
avg.	20.18	16.46	4.47
stdev	4.75	4.86	1.91
sterr	1.50	1.62	0.61
n	10.00	9.00	10.00

anti-Cx36 - NORMALIZED to wt avg.

	wt	gjd1a $^{dis3/+}$	gjd1a $^{dis3/dis3}$
avg. for animal	0.66	1.02	0.32
	0.96	1.10	0.30
	1.31	1.18	0.32
	1.26	0.74	0.36
	1.07	0.89	0.15
	1.01	0.70	0.18
	1.03	0.57	0.14
	1.19	0.58	0.08
	0.59	0.56	0.20
	0.92		0.17
avg.	1.00	0.82	0.22
stdev	0.24	0.24	0.09
sterr	0.07	0.08	0.03
n	10.00	9.00	10.00

gjd2a^{fh437} Δ5bp incross

anti-Cx36 - RAW pixel values

	wt	gjd2a $^{\Delta 5bp/+}$	gjd2a $^{\Delta 5bp/\Delta 5bp}$
avg. for animal	29.81	17.98	0.44
	32.29	18.96	0.67
	27.46	21.54	0.34
	41.13	29.28	0.23
	44.55	30.83	0.55
	23.70	23.46	0.56
avg.	33.16	23.68	0.47
stdev	8.09	5.33	0.16
sterr	3.30	2.17	0.07
n	6.00	6.00	6.00

anti-Cx36 - NORMALIZED to wt avg.

	wt	gjd2a $^{\Delta 5bp/+}$	gjd2a $^{\Delta 5bp/\Delta 5bp}$
avg. for animal	0.90	0.54	0.01
	0.97	0.57	0.02
	0.83	0.65	0.01
	1.24	0.88	0.01
	1.34	0.93	0.02
	0.71	0.71	0.02
avg.	1.00	0.71	0.01
stdev	0.24	0.16	0.00
sterr	0.10	0.07	0.00
n	6.00	6.00	6.00

gjd1b^{fh435} Δ8bp incross

anti-Cx36 - RAW pixel values

	wt	gjd1b $^{\Delta 8bp/+}$	gjd1b $^{\Delta 8bp/\Delta 8bp}$
avg. for animal	22.72	25.11	24.85
	24.31	33.51	35.30
	22.04	20.11	26.27
	31.42	27.71	9.65
	54.32	12.73	31.01
	23.45	47.98	41.40
	30.31	22.80	28.45
	34.43	11.40	27.84
avg.	30.38	25.17	28.10
stdev	10.72	11.78	9.19
sterr	3.79	4.17	3.25
n	8.00	8.00	8.00

anti-Cx36 - NORMALIZED to wt avg.

	wt	gjd1b $^{\Delta 8bp/+}$	gjd1b $^{\Delta 8bp/\Delta 8bp}$
avg. for animal	0.75	0.83	0.82
	0.80	1.10	1.16
	0.73	0.66	0.86
	1.03	0.91	0.32
	1.79	0.42	1.02
	0.77	1.58	1.36
	1.00	0.75	0.94
	1.13	0.38	0.92
avg.	1.00	0.83	0.93
stdev	0.35	0.39	0.30
sterr	0.12	0.14	0.11
n	8.00	8.00	8.00

gjd2b^{fh329} G42* incross

anti-Cx36 - RAW pixel values

	wt	gjd2b $^{G42*/+}$	gjd2b $^{G42*/G42*}$
avg. for animal	9.63	12.90	15.43
	12.55	34.04	20.47
	23.94	17.99	18.32
	22.26	30.71	10.53
	22.45	30.63	19.20
	15.15	18.67	24.68
	14.56	12.74	14.13
	13.24	22.98	28.71
avg.	16.72	22.58	18.94
stdev	5.38	8.36	5.82
sterr	1.90	2.96	2.06
n	8.00	8.00	8.00

anti-Cx36 - NORMALIZED to wt avg.

	wt	gjd2b $^{G42*/+}$	gjd2b $^{G42*/G42*}$
avg. for animal	0.58	0.77	0.92
	0.75	2.04	1.22
	1.43	1.08	1.10
	1.33	1.84	0.63
	1.34	1.83	1.15
	0.91	1.12	1.48
	0.87	0.76	0.85
	0.79	1.37	1.72
avg.	1.00	1.35	1.13
stdev	0.32	0.50	0.35
sterr	0.11	0.18	0.12
n	8.00	8.00	8.00

gjd2b^{fh456} Δ12bp incross

anti-Cx36 - RAW pixel values

	wt	gjd2b $^{\Delta 12bp/+}$	gjd2b $^{\Delta 12bp/\Delta 12bp}$
avg. for animal	29.49	43.29	28.68
	28.2	29	29.47
	29.42	18.66	28.66
	38.18		28.84
	34.58		28.47
	24.25		31.11
avg.	30.69	30.32	29.21
stdev	4.94	12.37	0.99
sterr	2.02	7.14	0.41
n	6.00	3.00	6.00

anti-Cx36 - NORMALIZED to wt avg.

	wt	gjd2b $^{\Delta 12bp/+}$	gjd2b $^{\Delta 12bp/\Delta 12bp}$
avg. for animal	0.96	1.41	0.93
	0.92	0.95	0.96
	0.96	0.61	0.93
	1.24		0.94
	1.13		0.93
	0.79		1.01
avg.	1.00	0.99	0.95
stdev	0.16	0.40	0.03
sterr	0.07	0.23	0.01
n	6.00	3.00	6.00

- for M/CoLo, each avg. for animal represents 12-16 individual M/CoLo synapses
- for Aud/M, each ave. for animal represents 8-12 individual Aud/M synapses
- n.d. = not determined

*** cx35.1 12bp deletion homozygous mutants had no qualitative effect on spinal cord synapses

Fig.3

Aud/M - club ending, hindbrain

	anti-Cx36 - RAW pixel values						anti-Cx36 - NORMALIZED to wt ave.					
		gjd1a $^{\Delta 8bp / \Delta 8bp}$						gjd1a $^{\Delta 8bp / \Delta 8bp}$				
	wt	**gjd2a $^{\Delta 5bp / \Delta 5bp}$**	**gjd1b $^{\Delta 8bp / \Delta 8bp}$**	**gjd2b $^{G42* / G42*}$**	**gjd1b $^{\Delta 8bp / \Delta 8bp}$; gjd2b $^{G42* / G42*}$**		**wt**	**gjd2a $^{\Delta 5bp / \Delta 5bp}$**	**gjd1b $^{\Delta 8bp / \Delta 8bp}$**	**gjd2b $^{G42* / G42*}$**	**gjd1b $^{\Delta 8bp / \Delta 8bp}$; gjd2b $^{G42* / G42*}$**
avg. for animal	26.37	2.78	4.49	8.73	9.34	avg. for animal	0.92	0.10	0.16	0.30	0.32
	30.2	2.01	8.39	7.06	8.67		1.05	0.07	0.29	0.25	0.30
	27.59	2.38	9.46	8.47			0.96	0.08	0.33	0.29	
	31		7.38	6.63			1.08		0.26	0.23	
	28.68		7.95	8.23			1.00		0.28	0.29	
avg.	28.77	2.39	7.53	7.82	9.01	avg.	1.00	0.08	0.26	0.27	0.31
stdev	1.88	0.39	1.86	0.92	0.47	stdev	0.07	0.01	0.06	0.03	0.02
sterr	0.84	0.22	0.83	0.41	0.34	sterr	0.03	0.01	0.03	0.01	0.01
n	5.00	3.00	5.00	5.00	2.00	n	5.00	3.00	5.00	5.00	2.00

M/CoLo - spinal cord

	anti-Cx36 - RAW pixel values						anti-Cx36 - NORMALIZED to wt ave.					
		gjd1a $^{\Delta 8bp / \Delta 8bp}$						gjd1a $^{\Delta 8bp / \Delta 8bp}$				
	wt	**gjd2a $^{\Delta 5bp / \Delta 5bp}$**	**gjd1b $^{\Delta 8bp / \Delta 8bp}$**	**gjd2b $^{G42* / G42*}$**	**gjd1b $^{\Delta 8bp / \Delta 8bp}$; gjd2b $^{G42* / G42*}$**		**wt**	**gjd2a $^{\Delta 5bp / \Delta 5bp}$**	**gjd1b $^{\Delta 8bp / \Delta 8bp}$**	**gjd2b $^{G42* / G42*}$**	**gjd1b $^{\Delta 8bp / \Delta 8bp}$; gjd2b $^{G42* / G42*}$**
avg. for animal	33.19	5.23	5.04	4.36	4.83	avg. for animal	0.93	0.15	0.14	0.12	0.14
	37.94	3.96	4.69	3.9	4.06		1.06	0.11	0.13	0.11	0.11
	36.11	2.35	5.04	4.85			1.01	0.07	0.14	0.14	
avg.	35.75	3.85	4.92	4.37	4.45	avg.	1.00	0.11	0.14	0.12	0.12
stdev	2.40	1.44	0.20	0.48	0.54	stdev	0.07	0.04	0.01	0.01	0.02
sterr	1.38	0.83	0.12	0.27	0.39	sterr	0.04	0.02	0.00	0.01	0.01
n	3.00	3.00	3.00	3.00	2.00	n	3.00	3.00	3.00	3.00	2.00

- for M/CoLo, each avg. for animal represents 12-16 individual M/CoLo synapses
- for Aud/M, each ave. for animal represents 8-12 individual Aud/M synapses

Fig.4

gjd1a^{fh436} Δ8bp incross

gjd1a 8bp (fh436) het incross

	CoLo / M neurobiotin ratio in each animal				CoLo / M neurobiotin ratio normalized to wt ave.		
	wt	**cx34.1 $^{\Delta 8bp / +}$**	**cx34.1 $^{\Delta 8bp / \Delta 8bp}$**		**wt**	**cx34.1 $^{\Delta 8bp / +}$**	**cx34.1 $^{\Delta 8bp / \Delta 8bp}$**
avg. for animal	0.97	0.82	0.11	avg. for animal	1.07	0.90	0.12
	0.80	0.93	0.12		0.88	1.02	0.13
	0.84	0.99	0.10		0.93	1.09	0.11
	0.72	0.92	0.02		0.79	1.01	0.02
	1.05	1.31	0.05		1.16	1.44	0.06
	0.51	0.59	0.02		0.56	0.65	0.02
	1.50	0.75			1.65	0.83	
	0.87				0.96		
avg.	0.91	0.90	0.07	avg.	1.00	0.99	0.08
stdev	0.29	0.22	0.05	stdev	0.32	0.25	0.05
sterr	0.10	0.08	0.02	sterr	0.11	0.09	0.02
n	8.00	7.00	6.00	n	8.00	7.00	6.00

gjd2a^{fh437} Δ5bp incross

gjd2a 5bp (fh437) het incross

	CoLo / M neurobiotin ratio in each animal				CoLo / M neurobiotin ratio normalized to wt ave.		
	wt	**cx35.5 $^{\Delta 5bp / +}$**	**cx35.5 $^{\Delta 5bp / \Delta 5bp}$**		**wt**	**cx35.5 $^{\Delta 5bp / +}$**	**cx35.5 $^{\Delta 5bp / \Delta 5bp}$**
ave. for animal	0.83	0.82	0.1	ave. for animal	0.77	0.76	0.09
	1.01	0.52	0.06		0.94	0.48	0.06
	1.37	0.76	0.07		1.28	0.71	0.07
	1.13	0.65	0.1		1.05	0.61	0.09
	0.71		0.24		0.66		0.22
	1.23		0.05		1.14		0.05
	1.24				1.15		
avg.	1.07	0.69	0.10	avg.	1.00	0.64	0.10
stdev	0.24	0.13	0.07	stdev	0.22	0.12	0.07
sterr	0.09	0.07	0.03	sterr	0.08	0.06	0.03
n	7.00	4.00	6.00	n	7.00	4.00	6.00

- each ave. represents 8-12 CoLo cell bodies compared to 2 M cell bodies

Fig.5

	gene	protein	peptide target*	species	antibody	reactivity of antibody against HeLa expressed Cx … zf Cx34.1*	zf Cx34.7*	zf Cx35.1*	zf Cx35.5*	in vivo reactivity on genotypes… wt	$gjd1a^{dis3/dis3}$	$gjd2a^{\Delta 5bp/\Delta 5bp}$	in vivo comments on staining in wt
Used in Fig.5	gjd1a	Cx34.1	VHPESKDDRECLDLKD	rb	P03_A04	+++	-	-	-	+++	-	-	All areas are marked - fore/mid lateral, mid lateral, mid medial, medial sweep, lateral sweep with blotches, M + hillock, seg homologues, bright down SC and at M/CoLos.
	gjd2a	Cx35.5	ESKELVSSNTKPAK	ms	P04_B12	-	-	-	+++	+++	- some left Aud/M**	-	Bright M circuit, hillocks, seg homologues; clear midbrain spots, fore/mid lateral is weaker; medial and lateral sweeps; strong down SC and at M/CoLos.
commercial antibody from Invitrogen													
Used in most Figs.	polyclonal antibody against human Cx36			rb	36-4600	+	+	+	+	+++	- some left Aud/M**	-	Areas marked - fore/mid lateral, mid lateral, mid medial, medial sweep, lateral sweep with blotches, M + hillock, seg homologues, bright down SC and at M/CoLos.

* constructs expressed in HeLa cells were ZfCx34.1-oxGFP-Ctin-N1, ZfCx34.8-EGFP, ZfCx35.1-EGFP, ZfCx35.5-moxGFP-N1

** Cx stain remaining at Aud/M synapse in *gjd1a/cx34.1* mutants is consistent with Cx35.5 pairing with an unknown "other" Cx at these synapses; all staining was lost from M/CoLo synapses in these mutants; see text

Fig.6

Presynaptic cell transplanted - Aud/M - hindbrain

gjd1a^{fh360} dis3 incross

Cx34.1 is not required presynaptically

Xplanted cell geno. donor	Aud pre +/+				Aud pre cx34.1 dis3 / +				Aud pre cx34.1 dis3 / dis3			
geno. host	+/+				+/+				+/+			
anti-Cx36	Xplant associated	GFP- host neighbor	Xplant / host	(Xplant/ host)	Xplant associated	GFP- host neighbor	Xplant / host	(Xplant/ host)	Xplant associated	GFP- host neighbor	Xplant / host	(Xplant/ host)
avg. for noted	20.16	19.26	1.05	0.07	38.68	45.9	0.84	-0.25	28.74	25.22	1.14	0.19
synapses in	30.37	28.76	1.06	0.08	46.06	50.82	0.91	-0.14	53.93	46.93	1.15	0.20
animal	27.87	21.12	1.32	0.40	27.46	25.89	1.06	0.08	60.06	61.43	0.98	-0.03
	35.9	40.75	0.88	-0.18	33.83	33.47	1.01	0.02	62.93	66.87	0.94	-0.09
	52.87	44.56	1.19	0.25					66.76	67.38	0.99	-0.01
	29.37	27.54	1.07	0.09					29.2	30.01	0.97	-0.04
									23.72	23.45	1.01	0.02
ave			1.09	0.12			0.96	-0.07			1.03	0.03
stdev			0.15	0.20			0.10	0.15			0.08	0.11
sterr			0.06	0.08			0.05	0.08			0.03	0.04
n			6.00	6.00			4.00	4.00			7.00	7.00

gjd2a^{fh437} Δ5bp incross

Cx35.5 is required presynaptically

Xplanted cell geno. donor	Aud pre +/+				Aud pre cx35.5 Δ5bp / +				Aud pre cx35.5 Δ5bp / Δ5bp			
geno. host	+/+				+/+				+/+			
anti-Cx36	GFP+ Xplant associated	GFP- host neighbor	Xplant / host	log2 (Xplant/ host)	GFP+ Xplant associated	GFP- host neighbor	Xplant / host	log2 (Xplant/ host)	GFP+ Xplant associated	GFP- host neighbor	Xplant / host	log2 (Xplant/ host)
avg. for noted	6.07	5.12	1.19	0.25	4.68	5.09	0.92	-0.12	0.01	5.11	0.00	-9.00
synapses in	3.5	4.36	0.80	-0.32	5.12	7.62	0.67	-0.57	0.06	9.97	0.01	-7.38
animal	8.69	7.93	1.10	0.13	2.9	3.13	0.93	-0.11	0.03	21.14	0.00	-9.46
	3.39	3.25	1.04	0.06	9.31	12.2	0.76	-0.39	0.12	14.32	0.01	-6.90
	3.27	3.25	1.01	0.01					0.05	6.73	0.01	-7.07
	6.47	5.11	1.27	0.34					1.14	14.43	0.08	-3.66
ave			1.07	0.08			0.82	-0.30			0.02	-7.24
stdev			0.16	0.23			0.12	0.22			0.03	2.05
sterr			0.07	0.09			0.06	0.11			0.01	0.84
n			6.00	6.00			4.00	4.00			6.00	6.00

Postsynaptic cell transplanted - Aud/M - hindbrain

Cx34.1 is required postsynaptically

Xplanted cell geno. donor	M post +/+				M post cx34.1 dis3 / +				M post cx34.1 dis3 / dis3			
geno. host	+/+				+/+				+/+			
anti-Cx36	Xplant associated	GFP- host neighbor	Xplant / host	(Xplant/ host)	Xplant associated	GFP- host neighbor	Xplant / host	(Xplant/ host)	Xplant associated	GFP- host neighbor	Xplant / host	(Xplant/ host)
avg. for noted	10.25	11.51	0.89	-0.17	5.82	5.67	1.03	0.04	1.47	10.41	0.14	-2.82
synapses in	10.8	11.83	0.91	-0.13	5.21	7.93	0.66	-0.61	2.13	9.59	0.22	-2.17
animal	14.47	14.84	0.98	-0.04	4.24	6.75	0.63	-0.67	11.86	61.33	0.19	-2.37
	14.76	11.6	1.27	0.35	7.26	12.69	0.57	-0.81	25.18	43.57	0.58	-0.79
	41.46	44.99	0.92	-0.12	56.03	69.9	0.80	-0.32	36.48	98.89	0.37	-1.44
	77.48	62.34	1.24	0.31					17.47	44.61	0.39	-1.35
	46.12	38.52	1.20	0.26								
ave			1.06	0.07			0.74	-0.47			0.32	-1.82
stdev			0.17	0.23			0.18	0.34			0.16	0.76
sterr			0.06	0.09			0.08	0.15			0.07	0.31
n			7.00	7.00			5.00	5.00			6.00	6.00

Cx35.5 is not required postsynaptically

Xplanted cell geno. donor	M post +/+				M post cx35.5 Δ5bp / +				M post cx35.5 Δ5bp / Δ5bp			
geno. host	+/+				+/+				+/+			
anti-Cx36	GFP+ Xplant associated	GFP- host neighbor	Xplant / host	log2 (Xplant/ host)	GFP+ Xplant associated	GFP- host neighbor	Xplant / host	log2 (Xplant/ host)	GFP+ Xplant associated	GFP- host neighbor	Xplant / host	log2 (Xplant/ host)
avg. for noted	31.28	29.99	1.04	0.06	6.88	6.43	1.07	0.10	19.93	19.77	1.01	0.01
synapses in	51.4	56.89	0.90	-0.15	17.15	14	1.23	0.29	23.67	27.69	0.85	-0.23
animal	52.2	55.12	0.95	-0.08	14.07	17.93	0.78	-0.35	74.31	81.12	0.92	-0.13
	56.78	51.96	1.09	0.13	69.88	80.61	0.87	-0.21	62.56	49.99	1.25	0.32
	92.2	103.64	0.89	-0.17	80.87	104.09	0.78	-0.36	42.75	45.66	0.94	-0.10
					77.49	96.1	0.81	-0.31	47.32	56.14	0.84	-0.25
ave			0.98	-0.04			0.92	-0.14			0.97	-0.06
stdev			0.09	0.13			0.18	0.27			0.15	0.21
sterr			0.04	0.06			0.08	0.11			0.06	0.09
n			5.00	5.00			6.00	6.00			6.00	6.00

- Xplant = transplant
- for Aud/M, each ave. for animal represents 1-6 individual presynaptic or 6 postsynaptic Xplant associated synapses compared to 6-11 host associated synapses

Fig.6

Presynaptic cell transplanted - M/CoLo - spinal cord

gid1a^{fh360} dis3 incross

Cx34.1 is not required presynaptically

Xplanted cell	M pre											
geno. donor	+/+				cx34.1 dis3 / +				cx34.1 dis3 / dis3			
geno. host	+/+											
anti-Cx36	GFP+ Xplant associated	GFP- host neighbor	Xplant / host	log2 (Xplant/ host)	GFP+ Xplant associated	GFP- host neighbor	Xplant / host	log2 (Xplant/ host)	GFP+ Xplant associated	GFP- host neighbor	Xplant / host	log2 (Xplant/ host)
avg. for noted	18.63	20.33	0.92	-0.13	5.65	5.23	1.08	0.11	19.22	17.5	1.10	0.14
synapses in	20.15	20.42	0.99	-0.02	9.99	12.65	0.79	-0.34	7.15	6.59	1.08	0.12
animal	7.12	7.01	1.02	0.02	22.39	21.87	1.02	0.03	10.01	10.79	0.93	-0.11
	7.66	6.56	1.17	0.22	21.46	18.86	1.14	0.19	7.4	6.93	1.07	0.09
	6.06	5.23	1.16	0.21	15.65	14.35	1.09	0.13	3.56	3.54	1.01	0.01
	5.12	5.1	1.00	0.01	6.58	6.81	0.97	-0.05	5.45	5.53	0.99	-0.02
					2.23	2.32	0.96	-0.06				
					5.64	6.58	0.86	-0.22				
avg.			1.04	0.05			0.99	-0.03			1.03	0.04
stdev			0.10	0.14			0.12	0.18			0.07	0.09
sterr			0.04	0.06			0.04	0.06			0.03	0.04
n			6.00	6.00			8.00	8.00			6.00	6.00

gid2a^{hi437} Δ5bp incross

Cx35.5 is required presynaptically

Xplanted cell	M pre											
geno. donor	+/+				cx35.5 Δ5bp / +				cx35.5 Δ5bp / Δ5bp			
geno. host	+/+											
anti-Cx36	GFP+ Xplant associated	GFP- host neighbor	Xplant / host	log2(Xplant/ host)	GFP+ Xplant associated	GFP- host neighbor	Xplant / host	log2(Xplant/ host)	GFP+ Xplant associated	GFP- host neighbor	Xplant / host	log2(Xplant/ host)
avg. for noted	6.59	6.52	1.01	0.02	6.49	8.17	0.79	-0.33	1.2	17.36	0.07	-3.85
synapses in	9.03	8.89	1.02	0.02	9.11	13.5	0.67	-0.57	0.78	12.59	0.06	-4.01
animal	8.75	9.42	0.93	-0.11	10.55	13.97	0.76	-0.41	0.14	9.07	0.02	-6.02
	9.92	8.35	1.19	0.25	3.15	4.34	0.73	-0.46	0.22	8.59	0.03	-5.29
	8.44	8.59	0.98	-0.03	5.89	7.69	0.77	-0.38	0.18	6.41	0.03	-5.15
	6.72	6.75	1.00	-0.01					1.36	9.37	0.15	-2.78
									0.37	3.21	0.12	-3.12
									0.61	5.79	0.11	-3.25
									0.45	6.22	0.07	-3.79
ave			1.02	0.02			0.74	-0.43			0.07	-4.14
stdev			0.09	0.12			0.05	0.09			0.04	1.11
sterr			0.04	0.05			0.02	0.04			0.01	0.37
n			6.00	6.00			5.00	5.00			9.00	9.00

Postsynaptic cell transplanted - M/CoLo - spinal cord

gid1a^{fh360} dis3 incross

Cx34.1 is required postsynaptically

Xplanted cell	CoLo post											
geno. donor	+/+				cx34.1 dis3 / +				cx34.1 dis3 / dis3			
geno. host	+/+											
anti-Cx36	GFP+ Xplant associated	GFP- host neighbor	Xplant / host	log2 (Xplant/ host)	GFP+ Xplant associated	GFP- host neighbor	Xplant / host	log2 (Xplant/ host)	GFP+ Xplant associated	GFP- host neighbor	Xplant / host	log2 (Xplant/ host)
avg. for noted	9.33	9.40	0.99	-0.01	4.65	9.93	0.47	-1.09	0.68	16.03	0.04	-4.56
synapses in	15.23	14.58	1.04	0.06	3.41	6.25	0.55	-0.87	0.98	22.21	0.04	-4.50
animal	27.69	27.45	1.01	0.01	2.99	7.35	0.41	-1.30	0.33	14.71	0.02	-5.48
	4.57	5.28	0.87	-0.21	4.94	11.14	0.44	-1.17	1.74	26.86	0.06	-3.95
	5.78	4.97	1.16	0.22	15.11	26.79	0.56	-0.83	2	27.37	0.07	-3.77
	3.7	3.37	1.10	0.13	16.06	24.66	0.65	-0.62	0.12	7.47	0.02	-5.96
	3.34	3.75	0.89	-0.17	6.19	10.34	0.60	-0.74	1.06	10.75	0.10	-3.34
					9.78	17.73	0.55	-0.86	0.37	27.24	0.01	-6.20
					11.3	21.01	0.54	-0.89	2.1	21.21	0.10	-3.34
									0.74	14.21	0.05	-4.26
									0.77	31.12	0.02	-5.34
									0.15	24.54	0.01	-7.35
avg.			1.01	0.01			0.53	-0.93			0.05	-4.84
stdev			0.11	0.15			0.08	0.22			0.03	1.24
sterr			0.04	0.06			0.03	0.07			0.01	0.36
n			7.00	7.00			9.00	9.00			12.00	12.00

gid2a^{hi437} Δ5bp incross

Cx35.5 is not required postsynaptically

Xplanted cell	CoLo post											
geno. donor	+/+				cx35.5 Δ5bp / +				cx35.5 Δ5bp / Δ5bp			
geno. host	+/+											
anti-Cx36	GFP+ Xplant associated	GFP- host neighbor	Xplant / host	log2(Xplant/ host)	GFP+ Xplant associated	GFP- host neighbor	Xplant / host	log2(Xplant/ host)	GFP+ Xplant associated	GFP- host neighbor	Xplant / host	log2(Xplant/ host)
avg. for noted	16.78	15.98	1.05	0.07	9.24	8.63	1.07	0.10	13.29	13.28	1.00	0.00
synapses in	12.69	13.79	0.92	-0.12	14.02	13.77	1.02	0.03	16.22	15.1	1.07	0.10
animal	13.75	12.51	1.10	0.14	12.62	11.76	1.07	0.10	10.97	10.41	1.05	0.08
	4.16	4.32	0.96	-0.05	12.92	12.19	1.06	0.08	16.44	15.16	1.08	0.12
	5.75	6.19	0.93	-0.11	12.22	12.57	0.97	-0.04	17.35	16.69	1.04	0.06
					13.5	14.11	0.96	-0.06	15.65	16.47	0.95	-0.07
					11.61	11.37	1.02	0.03	15.36	15.93	0.96	-0.05
					13.41	13.88	0.97	-0.05	11.83	14.12	0.84	-0.26
					15.24	15	1.02	0.02	15.76	14.2	1.11	0.15
					13.76	13.47	1.02	0.03	11.7	13.87	0.84	-0.25
									16.49	15.2	1.08	0.12
									11.6	11.48	1.01	0.02
									11.84	12.93	0.92	-0.13
									17.08	15.13	1.13	0.17
									9.62	10.01	0.96	-0.06
									10.08	10.33	0.98	-0.04
									12.81	12.8	1.00	0.00
ave			0.99	-0.01			1.02	0.02			1.00	0.00
stdev			0.08	0.11			0.04	0.06			0.09	0.13
sterr			0.04	0.05			0.01	0.02			0.02	0.03
n			5.00	5.00			10.00	10.00			17.00	17.00

Both pre and post transplanted - M/CoLo - spinal cord

gid1a^{fh360} dis3 incross

Cx34.1 loss from both pre and postsynaptic neurons is not additive

Xplanted cell	M & CoLo											
geno. donor	+/+				cx34.1 dis3 / +				cx34.1 dis3 / dis3			
geno. host	+/+											
anti-Cx36	GFP+ Xplant associated	GFP- host neighbor	Xplant / host	log2 (Xplant/ host)	GFP+ Xplant associated	GFP- host neighbor	Xplant / host	log2 (Xplant/ host)	GFP+ Xplant associated	GFP- host neighbor	Xplant / host	log2 (Xplant/ host)
avg. for noted	5.03	5.23	0.96	-0.06	7.32	9.93	0.74	-0.44	1.02	22.21	0.05	-4.44
synapses in	5.08	5.1	1.00	-0.01	3.38	7.35	0.46	-1.12	1.12	14.71	0.08	-3.72
animal					7.06	26.79	0.26	-1.92	0.55	27.37	0.02	-5.64
					6.06	10.34	0.59	-0.77	0.93	11.66	0.08	-3.65
					6.78	12.65	0.54	-0.90	0.09	6.59	0.01	-6.19
					10.01	18.86	0.53	-0.91	0.16	6.93	0.02	-5.44
avg.			0.98	-0.03			0.52	-1.01			0.04	-4.85
stdev			0.02	0.04			0.16	0.50			0.03	1.06
sterr			0.02	0.03			0.06	0.20			0.01	0.43
n			2.00	2.00			6.00	6.00			6.00	6.00

gid2a^{hi437} Δ5bp incross

Cx35.5 loss from both pre and postsynaptic neurons is not additive

Xplanted cell	M & CoLo											
geno. donor	+/+				cx35.5 Δ5bp / +				cx35.5 Δ5bp / Δ5bp			
geno. host	+/+											
anti-Cx36	GFP+ Xplant associated	GFP- host neighbor	Xplant / host	log2(Xplant/ host)	GFP+ Xplant associated	GFP- host neighbor	Xplant / host	log2(Xplant/ host)	GFP+ Xplant associated	GFP- host neighbor	Xplant / host	log2(Xplant/ host)
avg. for noted	6.49	6.52	1.00	-0.01	n.d.	n.d.	n.d.	n.d.	0.05	6.41	0.01	-7.00
synapses in	8.3	8.59	0.97	-0.05					0.16	3.21	0.05	-4.33
animal	6.11	6.75	0.91	-0.14								
ave			0.96	-0.07							0.03	-5.66
stdev			0.05	0.07							0.03	1.89
sterr			0.03	0.04							0.02	1.34
n			3.00	3.00							2.00	2.00

- Xplant = transplant
- for M/CoLo, each ave. for animal represents 8 individual presynaptic or 1-8 postsynaptic Xplant associated synapses compared to 8-12 host associated synapses
- n.d. = not determined

Fig.7 Postsynaptic cell transplanted - Aud/M - spinal cord

gid1a^{fh360} dis3 incross

Cx34.1 is sufficient postsynaptically

Xplanted cell geno. donor	M post +/+										
geno. host	+/+			cx34.1 $^{dis3 / +}$				cx34.1 $^{dis3 / dis3}$			
anti-Cx36	GFP+ Xplant associated	GFP- host neighbor	Xplant / host	GFP+ Xplant associated	GFP- host neighbor	Xplant / host	log2 (Xplant/ host)	GFP+ Xplant associated	GFP- host neighbor	Xplant / host	log2 (Xplant/ host)
avg. for noted	n.d.	n.d.	n.d.	n.d.	n.d.	n.d.	n.d.	5.37	1.09	4.93	2.30
synapses in								15.05	3.41	4.41	2.14
animal								15.1	2.81	5.37	2.43
								6.63	1.02	6.50	2.70
								10.91	1.5	7.27	2.86
								4.84	1.23	3.93	1.98
								9.33	1.77	5.27	2.40
ave										5.38	2.40
stdev										1.16	0.31
sterr										0.44	0.12
n										7.00	7.00

cx35.5^{fh437} Δ5bp incross

Cx35.5 is not sufficient postsynaptically

Xplanted cell geno. donor	CoLo post +/+										
geno. host	+/+			cx35.5 $^{Δ5bp / +}$				cx35.5 $^{Δ5bp / Δ5bp}$			
anti-Cx36	GFP+ Xplant associated	GFP- host neighbor	Xplant / host	GFP+ Xplant associated	GFP- host neighbor	Xplant / host	log2 (Xplant/ host)	GFP+ Xplant associated	GFP- host neighbor	Xplant / host	log2 (Xplant/ host)
avg. for noted	n.d.	n.d.	n.d.	n.d.	n.d.	n.d.	n.d.	0.04	0.03	1.33	0.42
synapses in								0.73	0.86	0.85	-0.24
animal								0.54	0.67	0.81	-0.31
								0.53	0.55	0.96	-0.05
								0.04	0.03	1.33	0.42
ave										1.06	0.05
stdev										0.26	0.35
sterr										0.12	0.16
n										5.00	5.00

- Xplant = transplant
- for Aud/M, each ave. for animal represents 1-6 individual presynaptic or 6 postsynaptic Xplant associated synapses compared to 6-11 host associated synapses
- n.d. = not determined

Fig.7

Presynaptic cell transplanted - M/CoLo - spinal cord

gid1a^{fh360} dis3 incross

Cx34.1 is not sufficent presynaptically

Xplanted cell	M pre									
geno. donor	+/+									
geno. host	+/+			cx34.1 dis3 / +				cx34.1 dis3 / dis3			
anti-Cx36	GFP+ Xplant associated	GFP- host neighbor	Xplant / host	GFP+ Xplant associated	GFP- host neighbor	Xplant / host	log2 (Xplant/ host)	GFP+ Xplant associated	GFP- host neighbor	Xplant / host	log2 (Xplant/ host)
avg. for noted	n.d.	n.d.	n.d.	2.95	3.47	0.85	-0.23	0.23	0.27	0.85	-0.23
synapses in				5.14	4.8	1.07	0.10	0.18	0.16	1.13	0.17
animal				6.11	5.1	1.20	0.26	0.14	0.13	1.08	0.11
				4.03	3.62	1.11	0.15	0.21	0.25	0.84	-0.25
				2.67	3.15	0.85	-0.24	0.28	0.38	0.74	-0.44
				4.25	2.76	1.54	0.62	0.09	0.12	0.75	-0.42
								0.22	0.13	1.69	0.76
ave						1.10	0.11			1.01	-0.04
stdev						0.26	0.33			0.34	0.43
sterr						0.10	0.13			0.13	0.16
n						6.00	6.00			7.00	7.00

Cx34.1 is sufficient postsynaptically

Xplanted cell	CoLo post									
geno. donor	+/+									
geno. host	+/+			cx34.1 dis3 / +				cx34.1 dis3 / dis3			
anti-Cx36	GFP+ Xplant associated	GFP- host neighbor	Xplant / host	GFP+ Xplant associated	GFP- host neighbor	Xplant / host	log2 (Xplant/ host)	GFP+ Xplant associated	GFP- host neighbor	Xplant / host	log2 (Xplant/ host)
avg. for noted	n.d.	n.d.	n.d.	5.59	3.23	1.73	0.79	8.14	0.25	32.56	5.03
synapses in				10.75	6.13	1.75	0.81	7.85	0.27	29.07	4.86
animal				7.51	4.5	1.67	0.74	12.52	0.26	48.15	5.59
				6.35	3.62	1.75	0.81	9.41	0.14	67.21	6.07
				4.11	2.31	1.78	0.83	7.59	0.18	42.17	5.40
								9	0.11	81.82	6.35
								11.79	0.28	42.11	5.40
								4.53	0.11	41.18	5.36
ave						1.74	0.80			48.03	5.51
stdev						0.04	0.04			17.83	0.50
sterr						0.02	0.02			6.30	0.18
n						5.00	5.00			8.00	8.00

Cx34.1 rescue from both pre and postsynaptic neurons is not additive

Xplanted cell	M & CoLo									
geno. donor	+/+									
geno. host	+/+			cx35.5 Δ5bp / +				cx35.5 Δ5bp / Δ5bp			
anti-Cx36	GFP+ Xplant associated	GFP- host neighbor	Xplant / host	GFP+ Xplant associated	GFP- host neighbor	Xplant / host	log2 (Xplant/ host)	GFP+ Xplant associated	GFP- host neighbor	Xplant / host	log2 (Xplant/ host)
avg. for noted	n.d.	n.d.	n.d.	6.49	4.24	1.53	0.61	5.35	0.25	21.40	4.42
synapses in				3.49	1.71	2.04	1.03	8.3	0.16	51.88	5.70
animal								8.95	0.18	49.72	5.64
ave						1.79	0.82			41.00	5.25
stdev						0.36	0.29			17.01	0.72
sterr						0.26	0.21			9.82	0.42
n						2.00	2.00			3.00	3.00

- Xplant = transplant
- for spinal cord, each avg. for host represents 8-16 individual M/CoLo synapses
- n.d. = not determined
- n.a. = not applicable

Postsynaptic cell transplanted - M/CoLo - spinal cord

cx35.5^{fh37} Δ5bp incross

Cx35.5 is sufficent presynaptically

Xplanted cell	M pre									
geno. donor	+/+									
geno. host	+/+			cx35.5 Δ5bp / +				cx35.5 Δ5bp / Δ5bp			
anti-Cx36	GFP+ Xplant associated	GFP- host neighbor	Xplant / host	GFP+ Xplant associated	GFP- host neighbor	Xplant / host	log2 (Xplant/ host)	GFP+ Xplant associated	GFP- host neighbor	Xplant / host	log2 (Xplant/ host)
avg. for noted	n.d.	n.d.	n.d.	3.49	2.22	1.57	0.65	8.6	0.66	13.03	3.70
synapses in				6.45	6.84	0.94	-0.08	8.42	0.57	14.77	3.88
animal				6.82	3.26	2.09	1.06	11.86	0.75	15.81	3.98
				7.18	3.37	2.13	1.09	10.85	0.65	16.69	4.06
				10.46	6.25	1.67	0.74	7.2	0.4	18.00	4.17
				5.6	3.32	1.69	0.75	11.86	0.39	30.41	4.93
				13.42	10.27	1.31	0.39	5.28	0.19	27.79	4.80
				6.95	3.94	1.76	0.82	6.66	0.21	31.71	4.99
				3.34	1.63	2.05	1.03	10.24	0.31	33.03	5.05
				6.65	4.04	1.65	0.72	9.92	0.47	21.11	4.40
ave						1.69	0.72			22.24	4.40
stdev						0.37	0.35			7.72	0.50
sterr						0.12	0.11			2.44	0.16
n						10.00	10.00			10.00	10.00

Cx35.5 is not sufficient postsynaptically

Xplanted cell	CoLo post									
geno. donor	+/+									
geno. host	+/+			cx35.5 Δ5bp / +				cx35.5 Δ5bp / Δ5bp			
anti-Cx36	GFP+ Xplant associated	GFP- host neighbor	Xplant / host	GFP+ Xplant associated	GFP- host neighbor	Xplant / host	log2 (Xplant/ host)	GFP+ Xplant associated	GFP- host neighbor	Xplant / host	log2 (Xplant/ host)
avg. for noted	n/d			8.11	7.96	1.02	0.03	0.24	0.26	0.92	-0.12
synapses in				7.06	7.13	0.99	-0.01	0.57	0.49	1.16	0.22
animal				8.8	7.48	1.18	0.23	0.57	0.41	1.39	0.48
				9.79	6.32	1.55	0.63	0.43	0.42	1.02	0.03
				3.74	3.61	1.04	0.05	1	0.83	1.20	0.27
				3.97	3.63	1.09	0.13	0.48	0.62	0.77	-0.37
				13.43	7.83	1.72	0.78	0.76	0.75	1.01	0.02
				2.47	2.95	0.84	-0.26	0.3	0.27	1.11	0.15
				2.14	1.89	1.13	0.18	0.02	0.02	1.00	0.00
				4.99	6.4	0.78	-0.36	0.01	0.02	0.50	-1.00
				3.03	3.16	0.96	-0.06	0.1	0.06	1.67	0.74
								0.04	0.1	0.40	-1.32
								0.81	0.95	0.85	-0.23
ave						1.12	0.12			1.00	-0.09
stdev						0.28	0.34			0.34	0.56
sterr						0.09	0.10			0.09	0.16
n						11.00	11.00			13.00	13.00

Cx35.5 rescue in both pre and postsynaptic neurons is not additive

Xplanted cell	M & CoLo									
geno. donor	+/+									
geno. host	+/+			cx35.5 Δ5bp / +				cx35.5 Δ5bp / Δ5bp			
anti-Cx36	GFP+ Xplant associated	GFP- host neighbor	Xplant / host	GFP+ Xplant associated	GFP- host neighbor	Xplant / host	log2 (Xplant/ host)	GFP+ Xplant associated	GFP- host neighbor	Xplant / host	log2 (Xplant/ host)
avg. for noted	n.d.	n.d.	n.d.	5.68	3.16	1.80	0.85	7.11	0.95	7.48	2.90
synapses in								2.03	0.05	40.60	5.34
animal								0.86	0.03	28.67	4.84
								1.81	0.06	30.17	4.91
ave						1.80	0.85			26.73	4.50
stdev						n.a.	n.a.			13.88	1.09
sterr						n.a.	n.a.			6.94	0.54
n						1.00	1.00			4.00	4.00

- Xplant = transplant
- for M/CoLo, each ave. for animal represents 8 individual presynaptic or 1-8 postsynaptic Xplant associated synapses compared to 8-12 host associated synapses
- n.d. = not determined

Fig.8

SLC react %

	gjd1a wt slbs	gjd1a -/dlbs	gjd2a wt slbs	gjd2a -/dlbs
avg. # SLC	20	90	100	70
in 10 trials*	100	100	100	60
per animal	90	100	87.5	40
	80	100	100	70
	90	80	70	22.2
	80	100	80	100
	70	100	30	70
	100	90	100	75
	100	70	66.7	50
	20	80	90	80
	40	90	40	71.4
	100	100	100	77.8
	90	100	70	55.6
	100	55.6	80	80
	90	50	77.8	33.3
	100	88.9	87.5	66.7
	100	90	100	33.3
	60	70	20	28.6
	80	100	60	100
	100	40	80	100
	37.5		44.4	100
	100		100	66.7
	11.1		100	100
	30		50	60
	70		55.6	87.5
	100			87.5
	70			90
				90
				10
avg.	75.13	84.73	75.58	68.12
stdev	29.30	18.54	24.30	25.44
sterr	5.64	4.14	4.86	4.72
n	27.00	20.00	25.00	29.00

* some trials are excluded if software cannot track movement**
** generally due to interference with the wall of the chamber

SLC latency

	gjd1a wt slbs	gjd1a -/dlbs	gjd2a wt slbs	gjd2a -/dlbs
time (ms) of	4	7	6	9
first move-	6	9	8	16
ment after	7	8	4	8
stimuls	6	8	5	7
	7	7	11	10
	7	8	3	7
	10	7	4	17
	5	8	3	7
	9	6	5	10
	8	12	8	8
	7	8	13	10
	4	12	7	9
	6	5	5	5
	7	5	8	6
	4	14	6	7
	5	13	12	6
	6	6	6	9
	4	15	10	7
	8	5	12	6
	5	5	8	9
	8	6	5	8
	6	7	8	9
	5	5	10	9
	6	10	6	4
	6	8	9	7
	7	5	7	8
	8	8	5	5
	9	13	7	7
	8	5	9	6
	8	14	6	7
	8	13	7	7
	7	15	8	6
	6	6	4	8
	8	9	3	8
	9	9	6	12
	6	9	7	7
	10	7	6	9
	8	9	7	6
	5	9	8	6
	6	6	8	10
	9	6	7	9
	6	10	6	14
	11	16	5	8
	16	7	7	10
	6	15	6	7
	8	6	7	15
	8	7	5	10
	6	12	4	8
	7	13	8	14
	7	11	9	14
	6	5	10	10
	4	5	7	5
	8	6	4	7
	6	14	4	8
	7	9	8	12
	5	6	7	10
	5	8	11	7
	8	10	9	9
	9	13	9	6
	9	8	6	9
	7	10	6	11
	8	16	8	8
	8	11	10	9
	6	12	7	5
	5	7	5	9
	8	5	4	9
	6	5	9	10
	9	8	6	9
	7	9	9	8
	8	9	4	7
	10	7	8	7
	9	10	6	6
	10	8	4	6
	10	12	9	8
	6	8	9	14
	7	4	7	5
	5	9	6	10
	3	7	9	5
	6	11	9	9
	7	9	9	9
	3	6	7	11
	9	12	6	9
	3	5	8	8
	5	10	6	8
	7	5	10	12
	8	8	7	8
	4	6	7	8
	10	4	5	10
	7	5	8	7
	5	5	4	7
	6	12	9	8
	4	9	9	16
	8	13	7	8
	8	6	6	12
	12	12	5	15
	9	14	3	9
	5	9	12	7
	11	8	5	9
	9	8	9	9
	11	9	5	9
	8	8	6	9
	7	8	5	11
	9	8	5	10
	6	10	8	7
	9	12	8	10
	4	10	8	9
	8	11	8	14
	6	9	5	8
	8	11	10	12
	5	10	7	8
	8	8	5	7
	7	8	4	8
	8	5	9	7
	9	4	4	7
	6	9	9	10
	5	8	3	12
	5	10	11	8
	6	9	7	12
	5	10	10	9
	6	8	11	11
	7	8	10	9
	7	9	6	9
	8	11	7	10
	5	8	10	8
	9	8	10	13
	7	8	8	7
	2	6	4	10
	6	7	9	8
	7	7	11	7
	11	5	3	7
	8	4	11	9
	8	5	4	12
	6	6	4	8
	5	10	5	15
	7	6	7	9
	6	9	8	6
	8	13	5	8
	8	8	4	7
	10	14	4	8
	6	15	4	6
	6	17	8	6
	5	11	4	9
	7	14	10	13
	4	6	8	8
	8	7	10	15
	7	15	9	8
	7	7	6	11
	6	11	8	8
	7	13	7	6
	5	7	8	7
	7	10	5	12
	4	5	9	10
	6	6	7	9
	6	11	5	6
	7	12	8	12
	8	14	8	8
	7	12	6	16
	9	8	10	6
	7	11	9	8
	6	16	6	11
	8		8	6
	10		7	8
	6		3	16
	10		7	14
	9		14	9
	6		16	9
	8		10	14
	7		11	11
	3		10	14
	6		14	12
	4		8	7
	7		10	7
	6			6
	8			10
	7			11
	4			8
	7			9
	8			13
	6			10
	9			13
	10			
	9			
	10			
	7			
	10			
	9			
avg.	7.03	8.92	7.25	9.05
stdev	1.96	3.06	2.46	2.64
sterr	0.14	0.24	0.19	0.20
n	186.00	160.00	172.00	180.00

SLC angle

bin	gjd1a wt slbs	gjd1a -/dlbs	gjd2a wt slbs	gjd2a -/dlbs
<30	0.00	1.86	0.00	1.11
30-50	0.53	5.59	2.91	6.11
50-70	0.00	8.07	1.74	6.67
70-90	4.79	8.70	5.23	5.56
90-110	9.57	8.70	18.02	8.33
110-130	33.51	15.53	38.95	21.67
130-150	31.38	27.95	21.51	29.44
150-170	11.17	13.66	8.14	11.67
170-190	4.26	3.73	2.33	6.11
190-210	2.66	2.48	0.58	1.67
>210	2.13	3.73	0.58	1.67
total	100.00	100.00	100.00	100.00

SLC max. angular velocity

bin	gjd1a wt slbs	gjd1a -/dlbs	gjd2a wt slbs	gjd2a -/dlbs
<18	2.72	16.77	3.18	12.07
19-20	7.07	14.84	14.01	9.20
21-22	14.67	12.26	31.21	17.82
23-24	27.72	21.29	19.75	24.14
25-26	20.11	15.48	14.65	15.52
27-28	10.33	5.81	6.37	8.05
29-30	6.52	4.52	3.82	1.72
31-32	4.89	3.23	2.55	1.15
33-34	2.17	0.65	0.00	1.72
35-36	0.54	0.00	0.64	1.15
>37	3.26	5.16	3.82	7.47
total	100.00	100.00	100.00	100.00